



Lunar Latitude and Terrain Radiator Sensitivity Study

Will Birmingham,

Greg Schunk, Brian Evans

MSFC/ EV34/ Jacobs Space Exploration Group/ESSCA Contract

Presented By

William Birmingham



Thermal & Fluids Analysis Workshop

TFAWS 2024

August 26-30, 2024

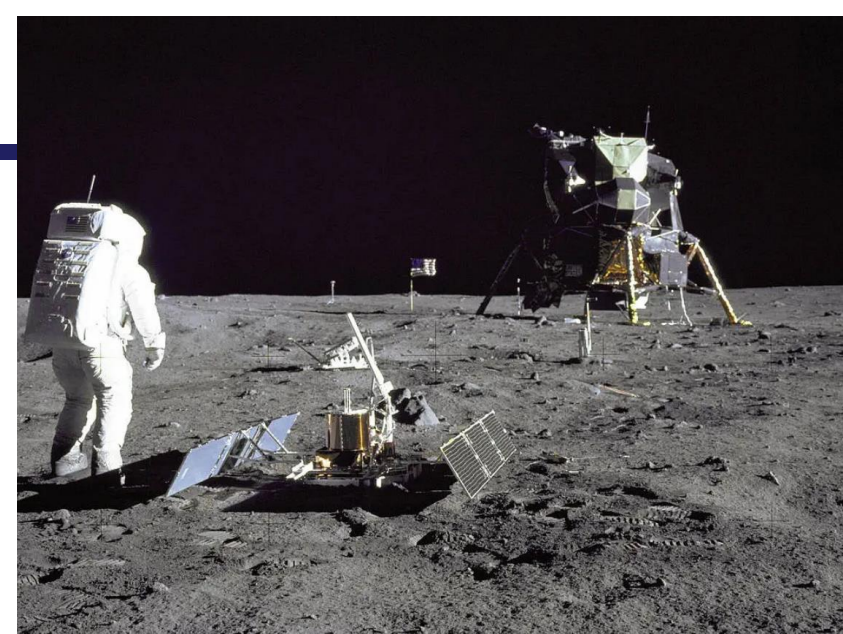
NASA Glenn Research Center

Cleveland, OH



Introduction

- As the number of planned lunar missions continues to grow, so also does the need for early-stage mission planning tools.
- Thermal design is especially sensitive to early phase decision making due to the highly integrated nature of thermal systems.
- The goal of this analysis is to create a set of early design-phase radiator scaling tools for lunar habitations or vehicles given basic lunar environmental characteristics.
- For this assessment, two parameters are selected for their unique utility in sizing radiators:
 - Relative terrain roughness
 - Lunar latitude

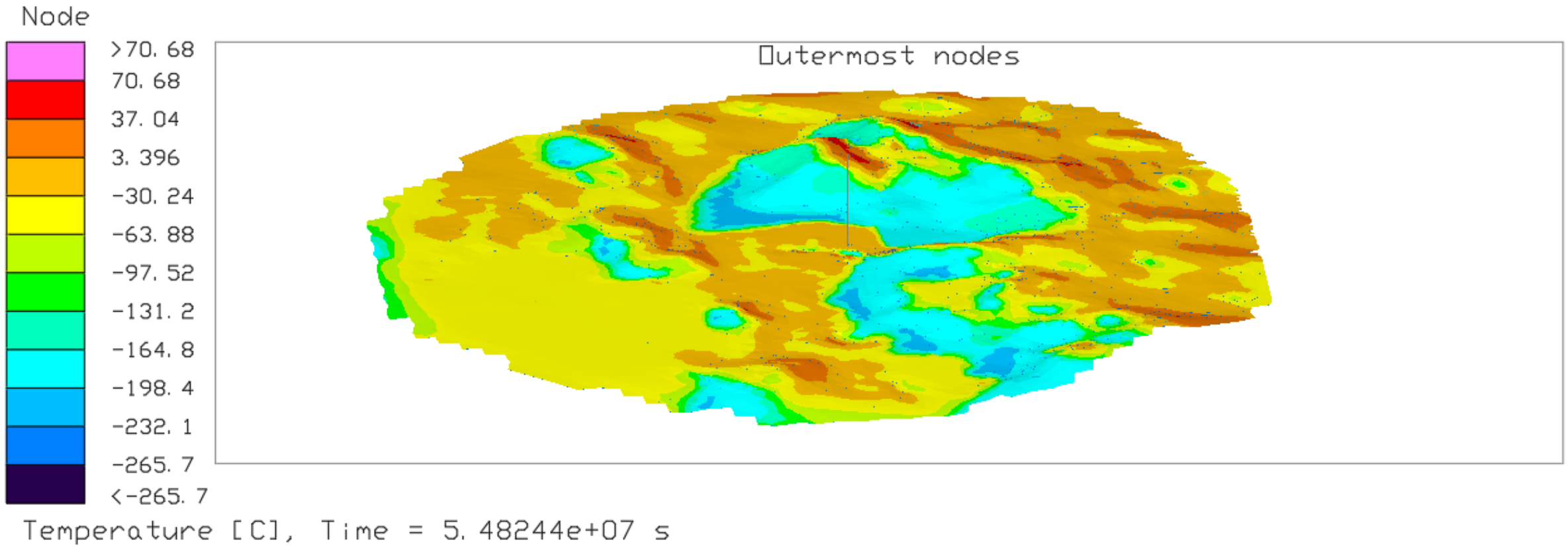


Apollo 11 Landing Site [1]



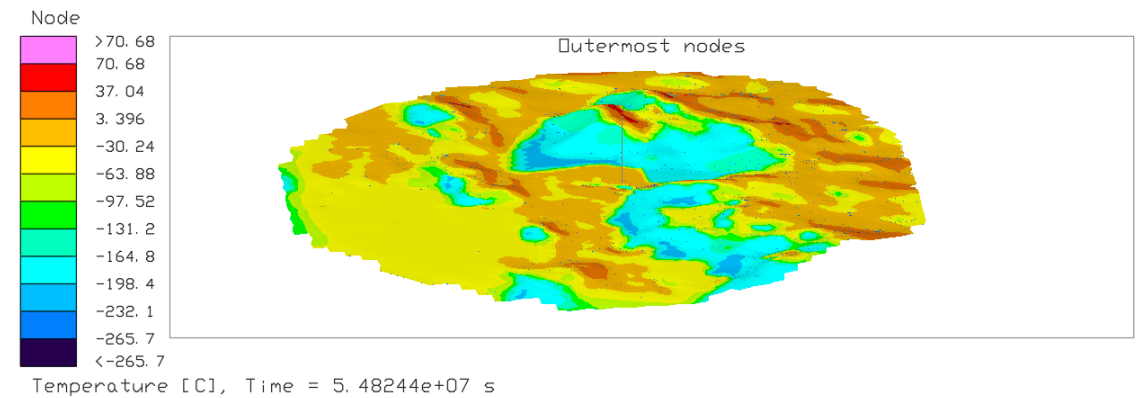
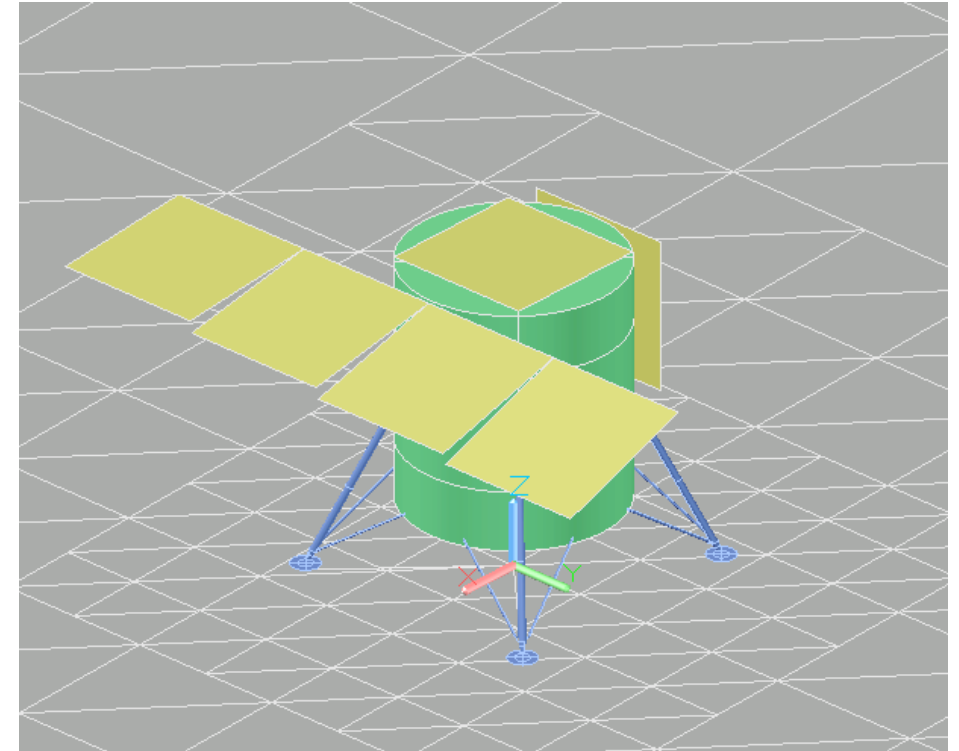
Apollo 15 Landing Site₂[2]

Part 1: Terrain Sensitivity Study



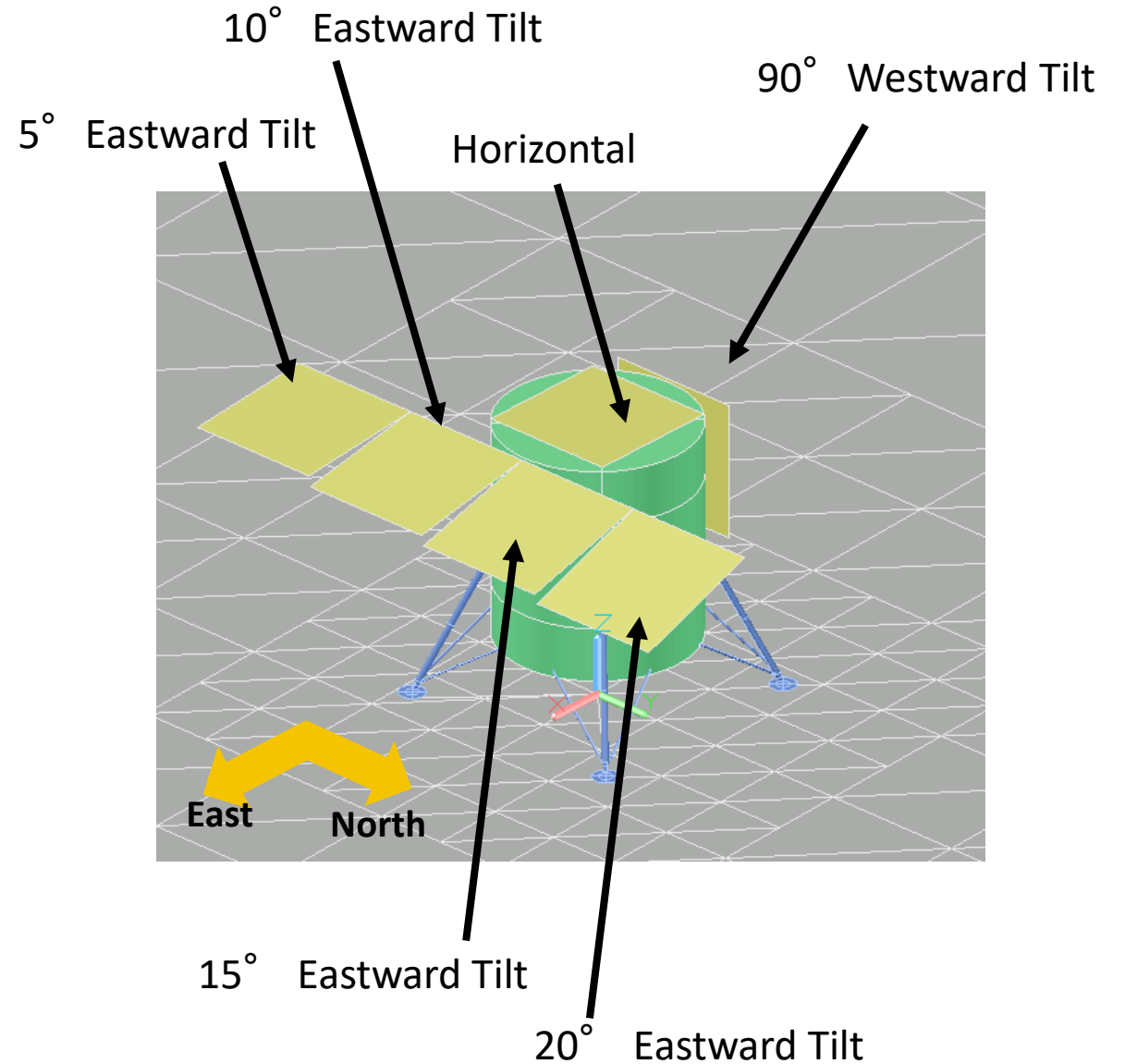
The goals of the terrain sensitivity study are to:

- Determine the thermal impact of terrain features on radiator performance decoupled from latitude effects.
- Estimate radiator performance degradation at different orientations/tilt angles during a full equatorial lunar day. Considering tilt allows for determination of sensitivity to imperfections in lander or radiator orientation.
- Utilize a thermal model with a simplified generic lunar lander and detailed terrain mesh to allow for rapid assessment of radiator behavior in different environments.



■ Radiators:

- All radiators are 10m^2 ($3.162\text{m} \times 3.162\text{m}$).
- Two sets of cases are analyzed: one set with all radiators at 10°C , and one set with radiators at 60°C .
- Radiation calculations are turned off for the radiator undersides (radiator underside coatings are studied in Part 2).
- Six radiators are modeled:
 - Horizontal upward facing
 - Vertical westward facing
 - 5° eastward tilt
 - 10° eastward tilt
 - 15° eastward tilt
 - 20° eastward tilt



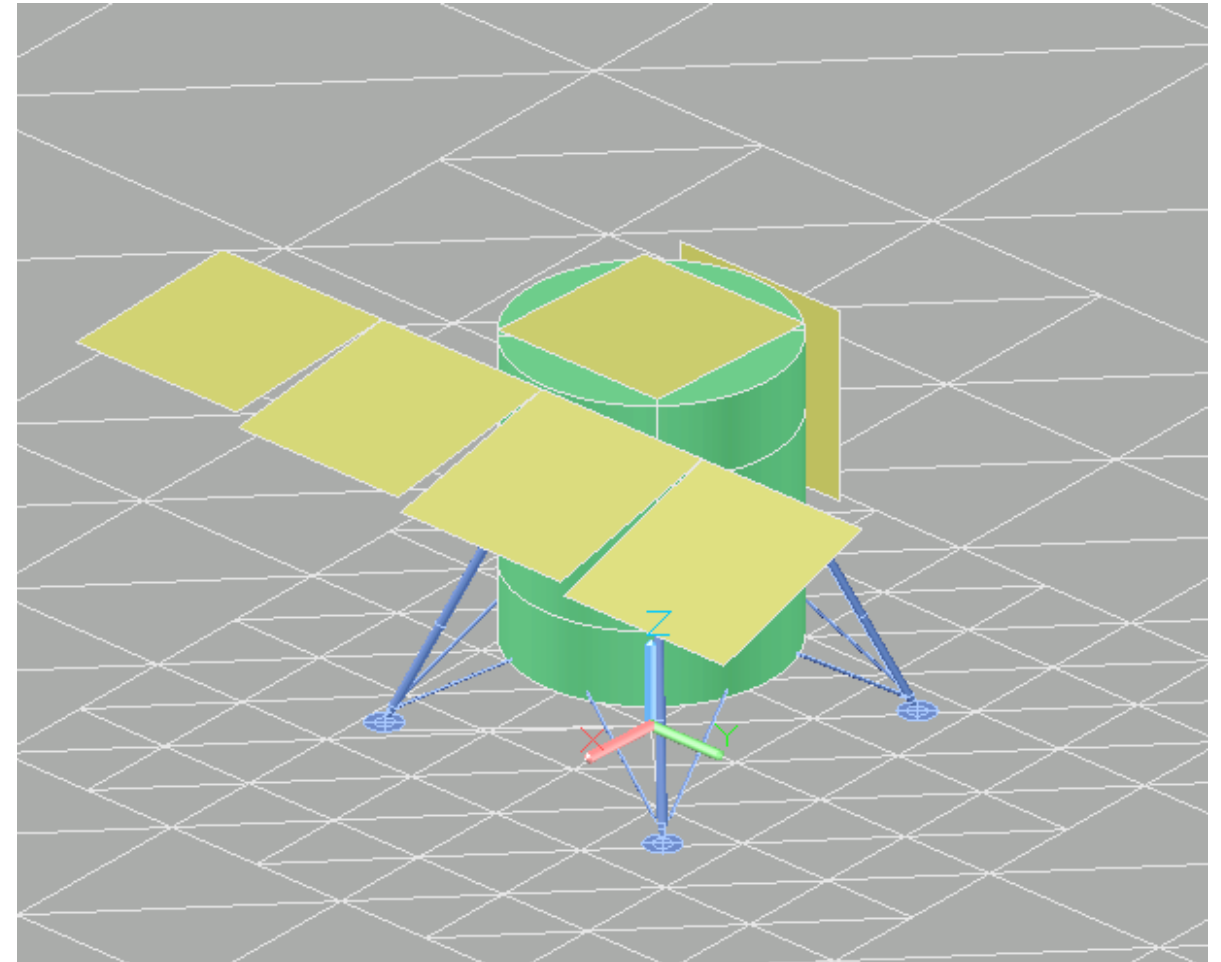
■ Lander Module:

- Main structure is an enclosed cylinder: 4.5m diameter, 5m tall.
- The walls are convectively coupled to a 20°C bulk gas node.
- Lander legs position the main cylinder ~1.5m off the ground.
- The main goal of the lander is to create reasonable and realistic shadows/reflections on the regolith.

■ Optical properties:

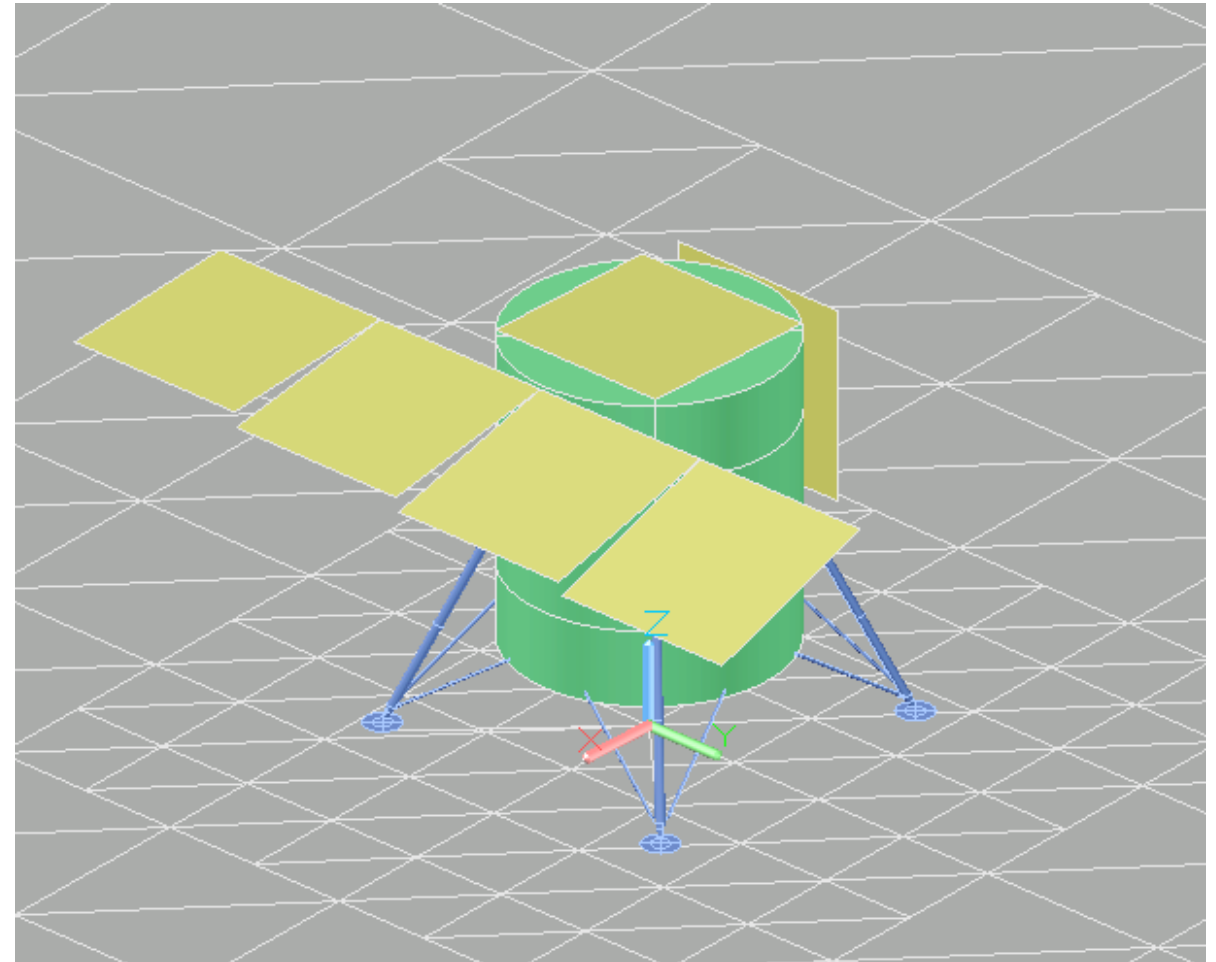
- Cylindrical Structure: Beta Cloth ($\alpha/\epsilon=0.3/0.9$).
- Lander legs: Silver Teflon ($\alpha/\epsilon=0.08/0.81$).
- Radiator top/out: Generic low absorptance white paint ($\alpha/\epsilon=0.09/0.91$) [3].
- Radiator bottom/in: Not in analysis (note underside conditions are studied in Part 2).
- Regolith: Highland optical properties used are: $\alpha/\epsilon = 0.84/0.98$, and mare optical properties used are $\alpha/\epsilon = 0.93/0.98$ [4].

Note: regolith optical properties used are consistent with the regolith type found at each site.



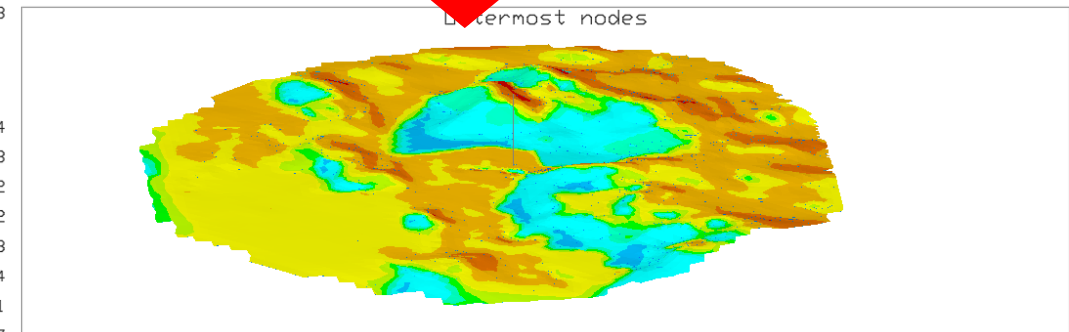
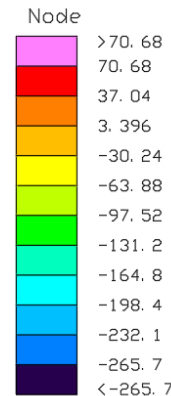
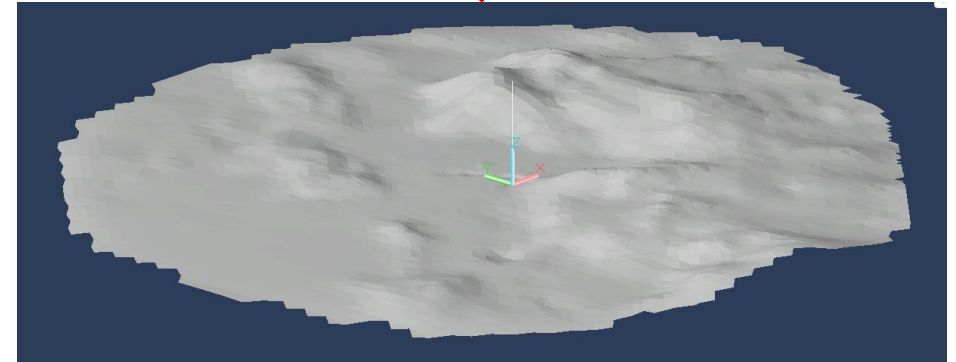
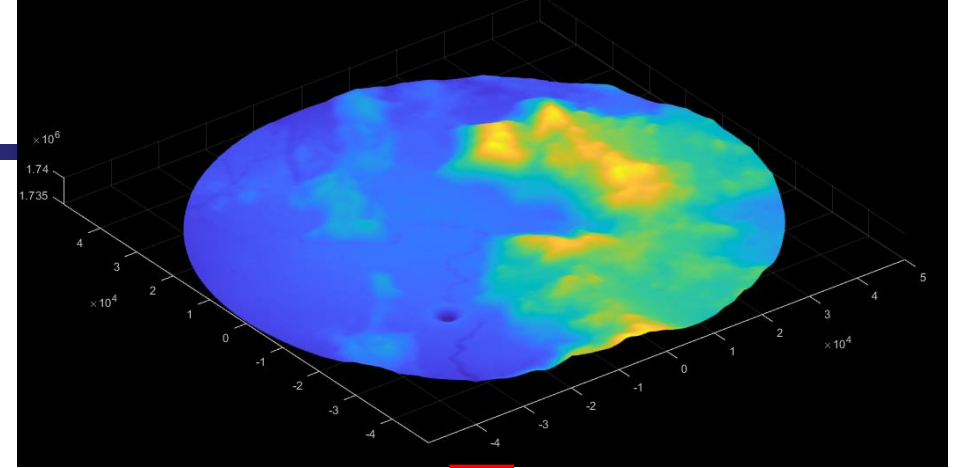
- Thermophysical properties:
 - Lander structure, legs, and radiators: 6061 T6 Aluminum.
 - Regolith: thermophysical properties obtained from the Human Landing System (HLS) Lunar Thermal Analysis Guidebook (LTAG) [5].
- Insulation:
 - Lander structure: $\epsilon^*=0.01$.
 - Lander legs: $\epsilon^*=0.03$.
 - Radiator backside: **NONE - backside excluded from radiation calculation.**
 - Regolith: Regolith depth & thermal mass is modeled using insulation stack applied to the back/under side (per LTAG recommendation) [5].

Layer #	Thickness (m)	Density (kg/m ³)
Layer 1	0.2614	1723
Layer 2	0.3369	1723
Layer 3	0.504	1800
Layer 4	0.8877	1800



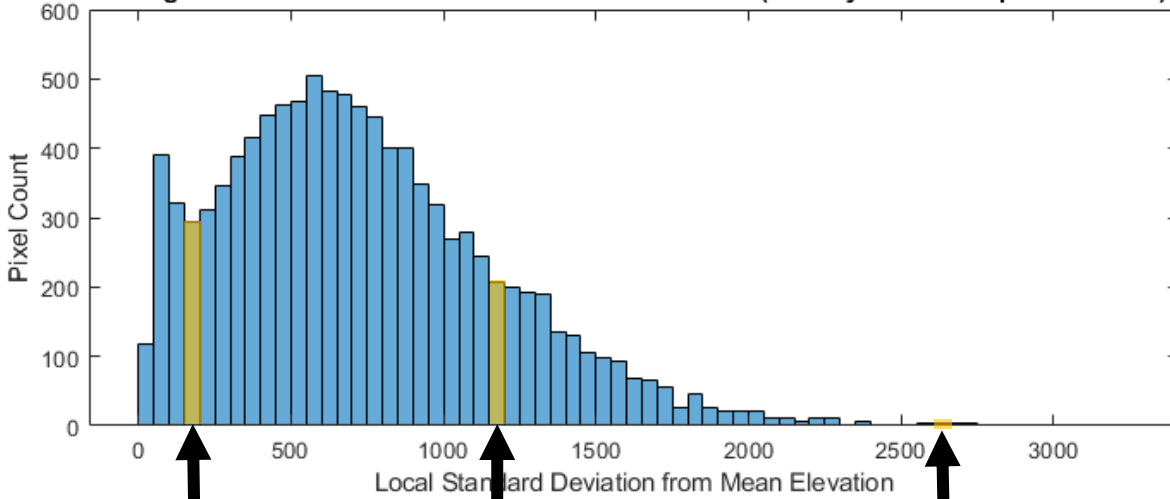
■ Terrain Mesh:

- Cylindrical projections of **lunar digital elevation maps** (LDEM) are extracted at maximum resolution (~60m per pixel) from an MIT-hosted planetary data system (PDS) node: https://imbrium.mit.edu/BROWSE/LOLA_GDR/CYLINDRICAL/ELEVATION/
- Cylindrical LDEMs are converted to point cloud x,y,z vectors using **MATLAB**. MATLAB also isolates a 100km diameter section of terrain around the landing site of interest
- **MeshLab** is used to convert the point cloud to a mesh with higher density near the vehicle
- The MeshLab meshes can be imported directly into AutoCad/Thermal Desktop as a DXF, and can be manipulated further from there



Temperature [C], Time = 5.48244e+07 s

Histogram of Standard Deviation From Mean Elevation (Raw Cylindrical Map Pixel Count)

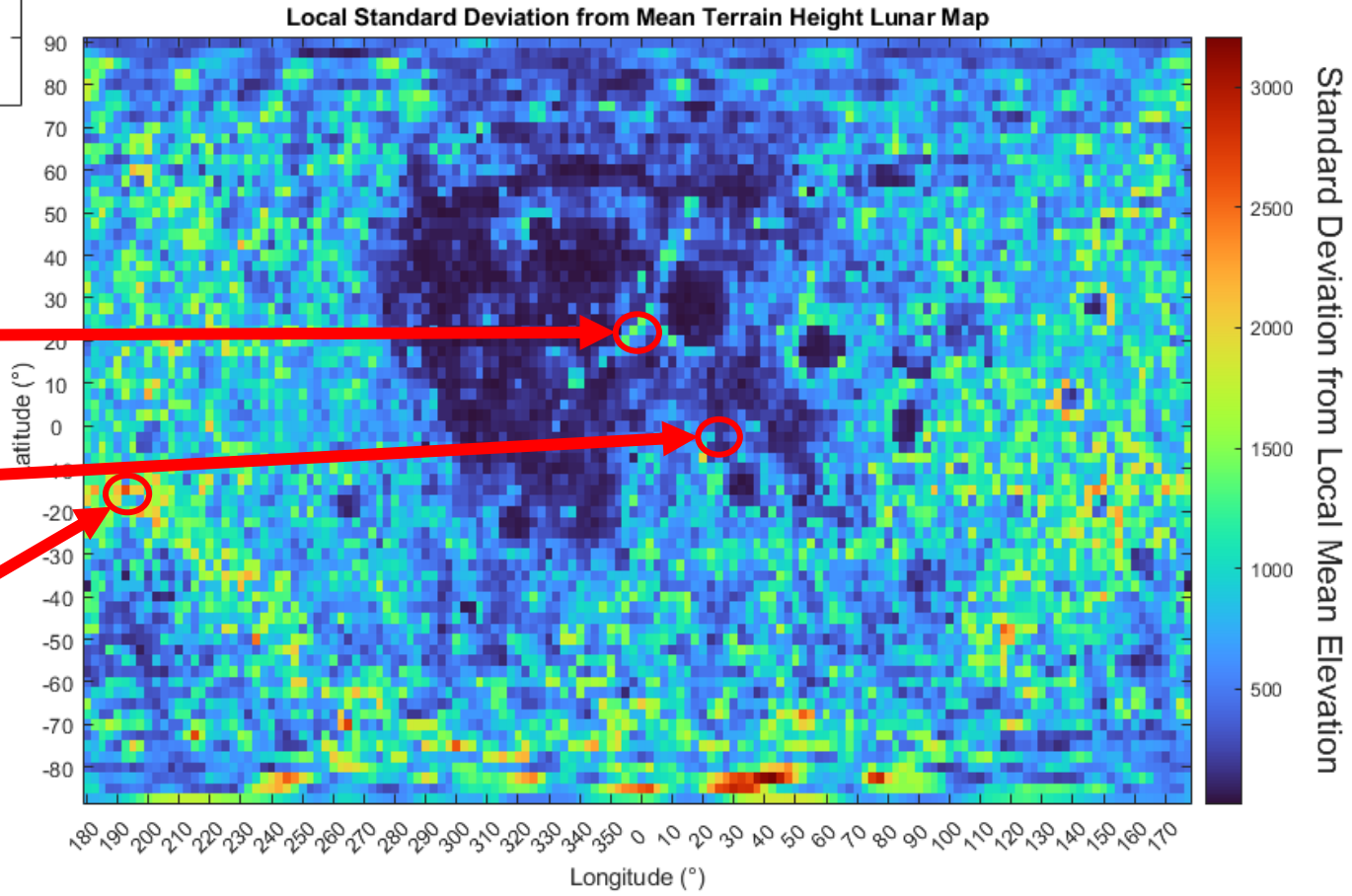


- Local elevation standard deviation is an approximate way to quantify the “roughness” of the lunar terrain.
- Each pixel in the map is ~76km X 76km at the equator.

Flat Terrain Sample (Apollo 11) *9th percentile*

Sparse Mountainous Terrain Sample (Apollo 15) *77th percentile*

Dense Mountainous Terrain Sample *99.8th percentile*

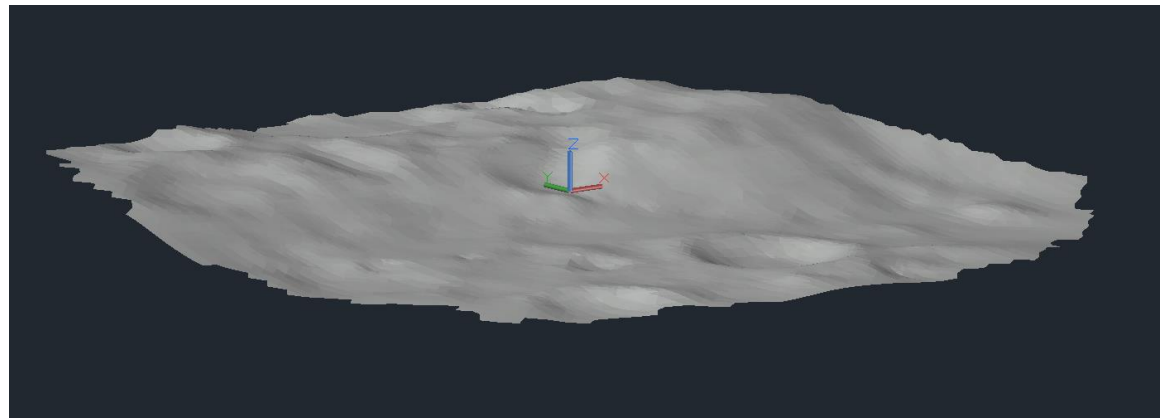
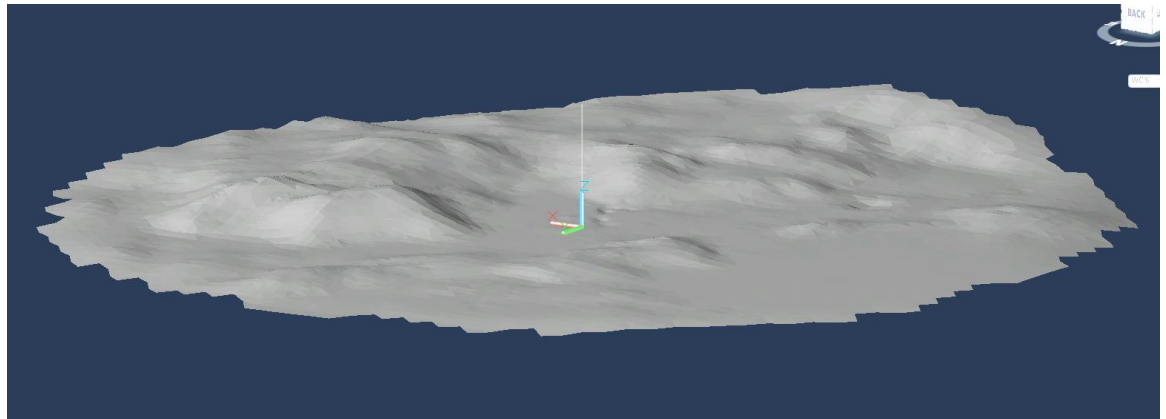
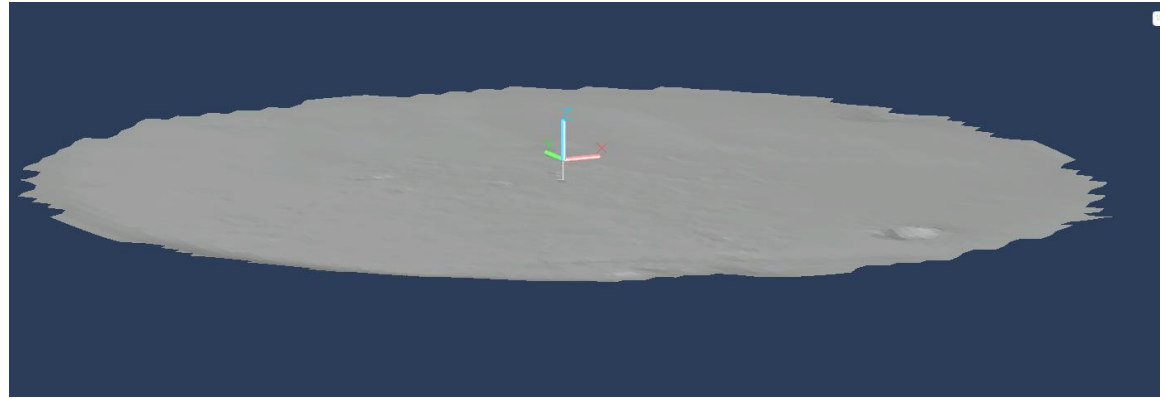


Note: the histogram shows the raw pixel count of the cylindrical map projection (it is not area weighted), so terrain at the poles is over-represented.

- **Flat Terrain Sample:**
 - Apollo 11 terrain is used for this case.
 - Very flat and featureless (closest approximation to an infinite plane).

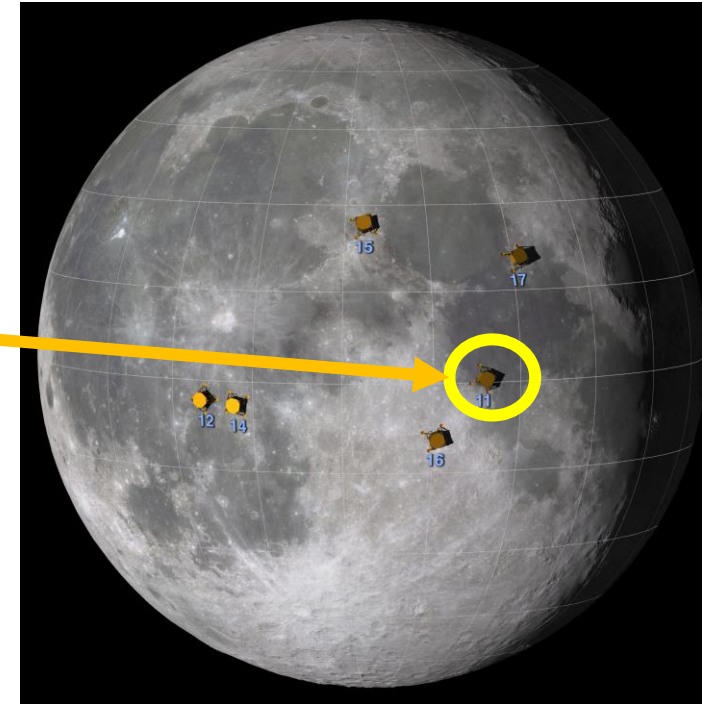
- **Sparse Mountainous Terrain Sample:**
 - Apollo 15 terrain is used for this case.
 - Tall mountains define the horizon with flat terrain in the immediate vicinity. Nearby mountains rise ~3km above the lander location.

- **Dense Mountainous Terrain Sample:**
 - A map of local standard deviation from mean height identified a highly mountainous section of terrain in a mid-latitude zone on the far side of the moon.
 - This location is in close proximity to very tall mountains, rising ~5km above the lander location. The lander sits in the bottom of a bowl (i.e. the horizon elevation is positive in all directions).



■ Solar Data:

- To decouple results from latitude effects, **the same solar path is used for all three analysis cases.**
- Even though terrain samples are pulled from different latitudes, **the solar path used for all cases is calculated from the perspective of the Apollo 11 site only.**
- Note latitude sensitivity is analyzed in part 2 of this study.

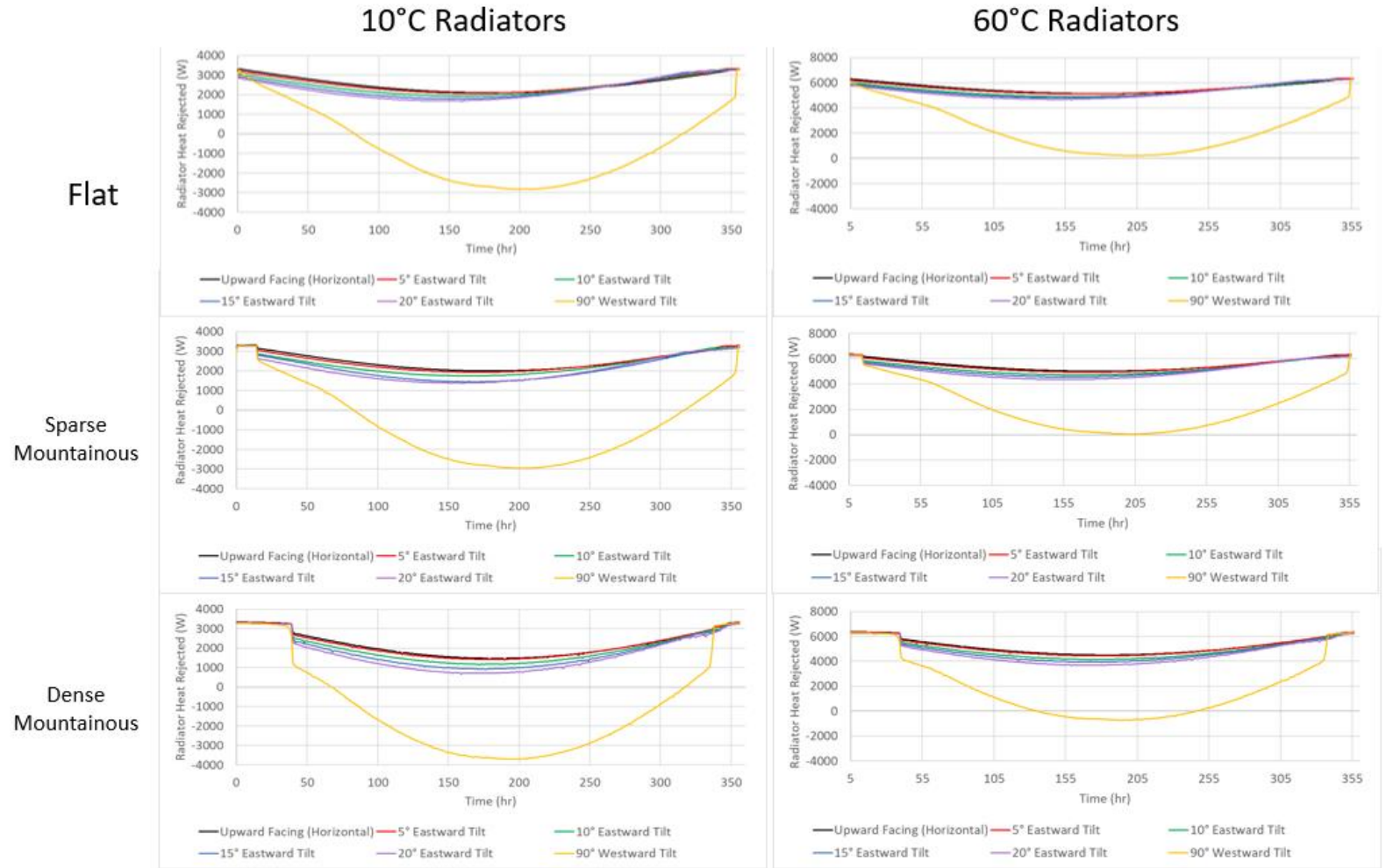


■ STK:

- Several years of solar vector data is calculated for the Apollo 11 landing site using STK.
- Excel is used to put the solar vector data in a TD-friendly format and divide the data into two sections:
 - **Transient Initializer:** Approximately 2 years of coarse (48 hour) solar position data that allows the top layer of the regolith to reach dynamic equilibrium. Ends when the lunar day of interest begins.
 - **Lunar Day:** 1 full lunar day at 1 hour increments.

Apollo Mission	Landing Date	Location	Latitude	Longitude	Duration	Peak Sun Angle	Estimated Surface Temperature
			(deg)	(deg)	(hrs)	(deg)	(K)
11	20-Jul-69	Mare Tranquillitatis	0.674 N	23.473 E	22	12.6	260.8
12	19-Nov-69	Oceanus Procellarum	3.013 S	23.422 W	31	25.9	310.2
14	5-Feb-71	Fra Mauro	3.646 S	17.472 W	34	29.9	320.6
15	30-Jul-71	Hadley Rille	26.132 N	3.633 E	67	34.2	330.4
16	21-Apr-72	Descartes	8.973 S	15.501 E	71	49.3	356.1
17	11-Dec-72	Taurus-Littrow	20.191 N	30.772 E	75	37.6	337.3

- As the sun rises, the radiator heat rejection slowly decreases until peak solar heating occurs, after which the heat rejection increases again as the sun sets.
- For the sparse and dense mountainous terrain samples, the heat rejection drops quickly shortly after the sun rises. This is due to the sun being obscured by terrain early in the morning.
- Using these curves, the **minimum** heat rejection can be determined, and this is used as the characteristic worst-case heat rejection.



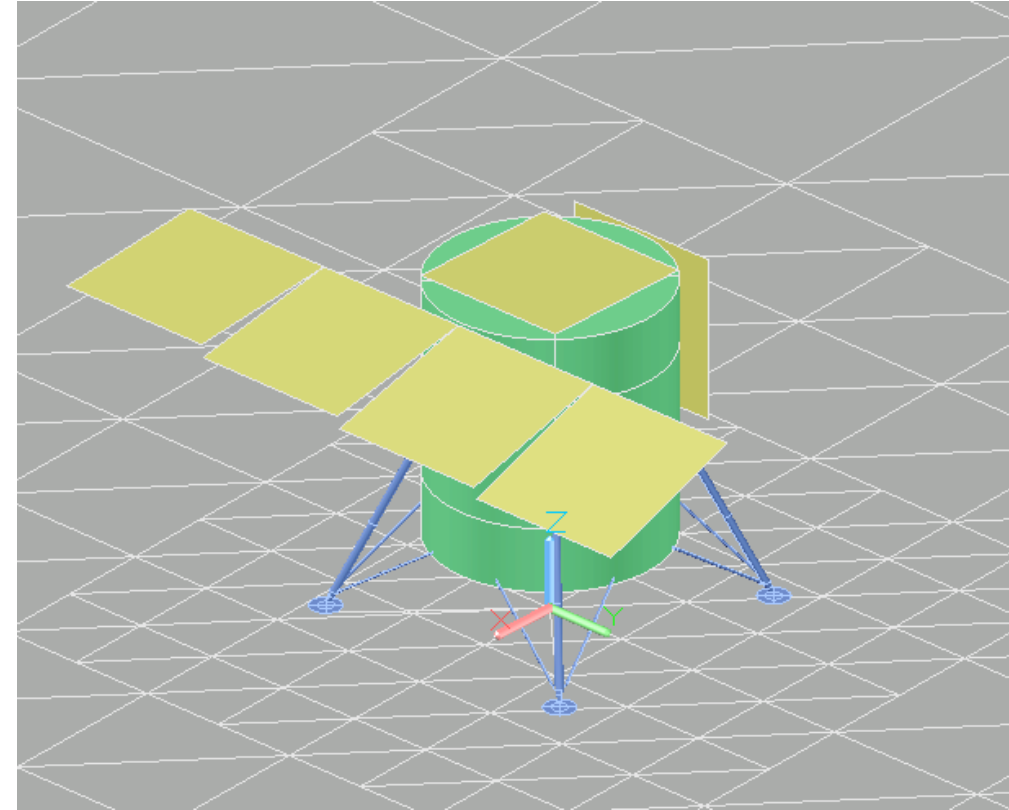
10° C Radiators

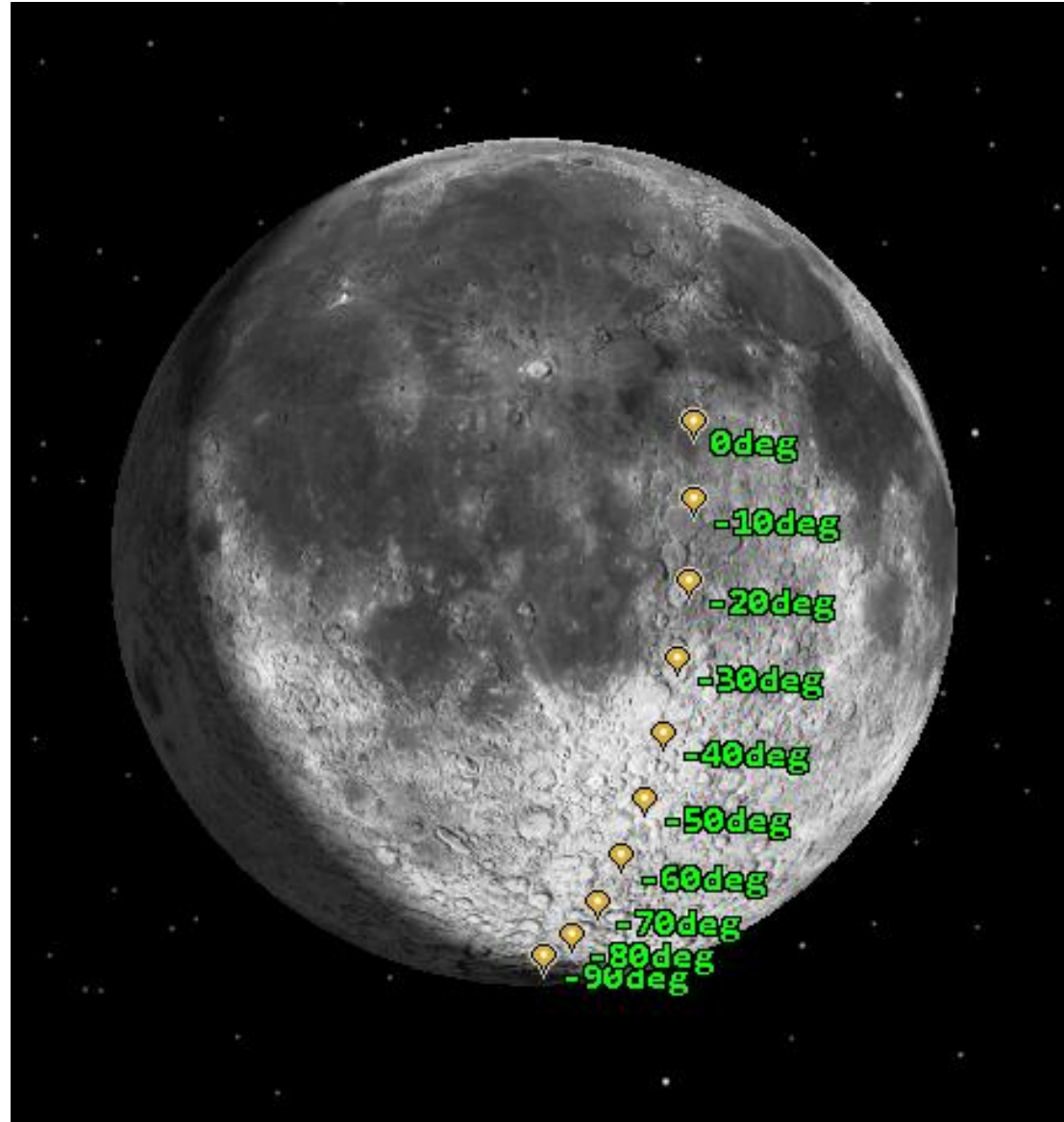
Ideal, Flat Terrain, Horizontal Radiator Heat Rejection (Control): 210W/m2	Flat Terrain: Percent Radiator Heat Rejection Decrease Due to <u>Tilt Alone</u>	Sparse Mountainous Terrain: Percent Radiator Heat Rejection Decrease Due to <u>Terrain and Tilt</u>	Dense Mountainous Terrain: Percent Radiator Heat Rejection Decrease Due to <u>Terrain and Tilt</u>
Horizontal Radiator	N/A	6%	30%
5° Eastward Tilt	1%	9%	33%
10° Eastward Tilt	8%	17%	46%
15° Eastward Tilt	14%	25%	55%
20° Eastward Tilt	21%	34%	68%

60° C Radiators

Ideal, Flat Terrain, Horizontal Radiator Heat Rejection (Control): 513W/m2	Flat Terrain: Percent Radiator Heat Rejection Decrease Due to <u>Tilt Alone</u>	Sparse Mountainous Terrain: Percent Radiator Heat Rejection Decrease Due to <u>Terrain and Tilt</u>	Dense Mountainous Terrain: Percent Radiator Heat Rejection Decrease Due to <u>Terrain and Tilt</u>
Horizontal Radiator	N/A	2%	13%
5° Eastward Tilt	0.4%	4%	13%
10° Eastward Tilt	4%	8%	19%
15° Eastward Tilt	6%	11%	23%
20° Eastward Tilt	9%	15%	29%

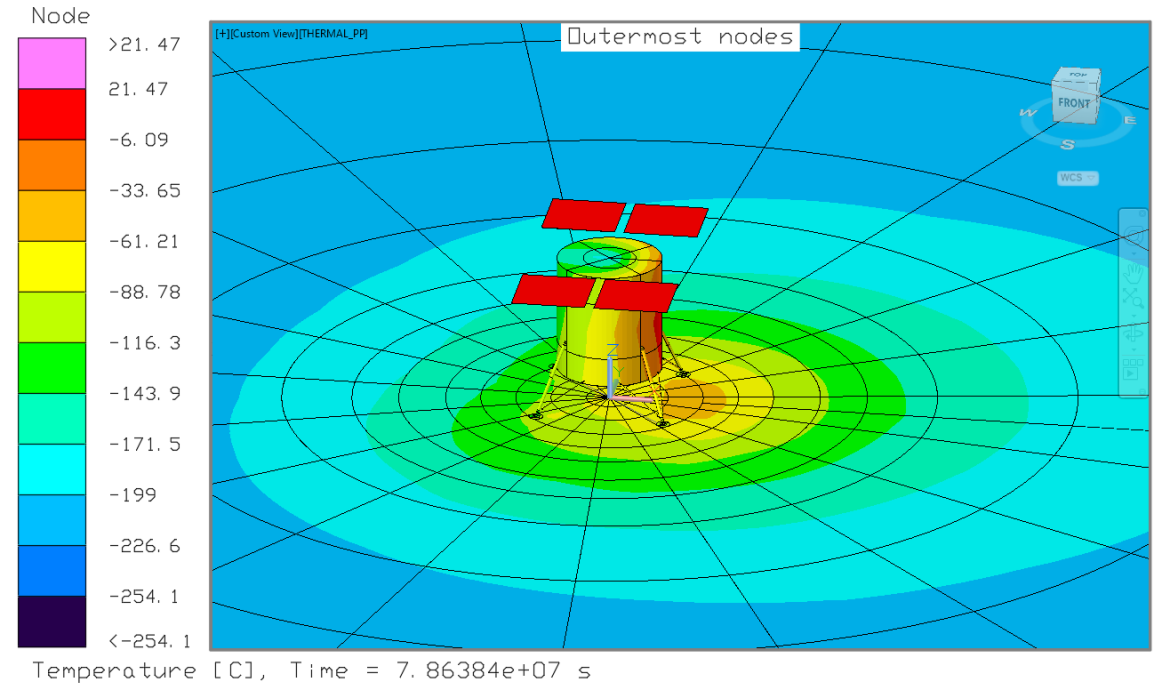
1. In an extreme worst-case hot scenario, highly mountainous terrain can have a significant impact on radiator performance.
 - **Dense mountainous terrain caused radiator performance degradation by 30% for a perfectly horizontal radiator.**
 - **Dense mountainous terrain coupled with a 20° tilt caused radiator performance to degrade by a maximum of 70% compared to a horizontal radiator on flat terrain.**
2. For landing sites with sparse mountains, impacts can be much more modest.
 - **Sparse mountainous terrain caused radiator performance degradation by 6% for a perfectly horizontal radiator.**
 - **Sparse mountainous terrain coupled with a 20° tilt caused radiator performance to degrade by a maximum of 37% compared to a horizontal radiator on flat terrain.**
3. **Horizontal radiators were found to be the superior configuration in both mountainous and flat terrain.**
4. For equatorial environments, **vertical radiators are highly ineffective regardless of the terrain.** The high regolith temperature results in the radiators absorbing rather than rejecting heat.
5. These degradation factors allow for quick worst-case approximations of terrain effects on a 10° C or 60° C radiator given the performance of the ideal case is known.





- Having determined the superior performance of horizontal radiators in extreme hot equatorial environments in Part 1, the goals of Part 2 are to:
 - Determine how the heat rejection capacity of horizontal radiators changes with latitude.
 - Determine how underside coatings on deployable horizontal radiators affects radiator performance at different latitudes.

- Decouple the latitude study from location-specific terrain effects by using a perfectly flat disk to represent the lunar surface.



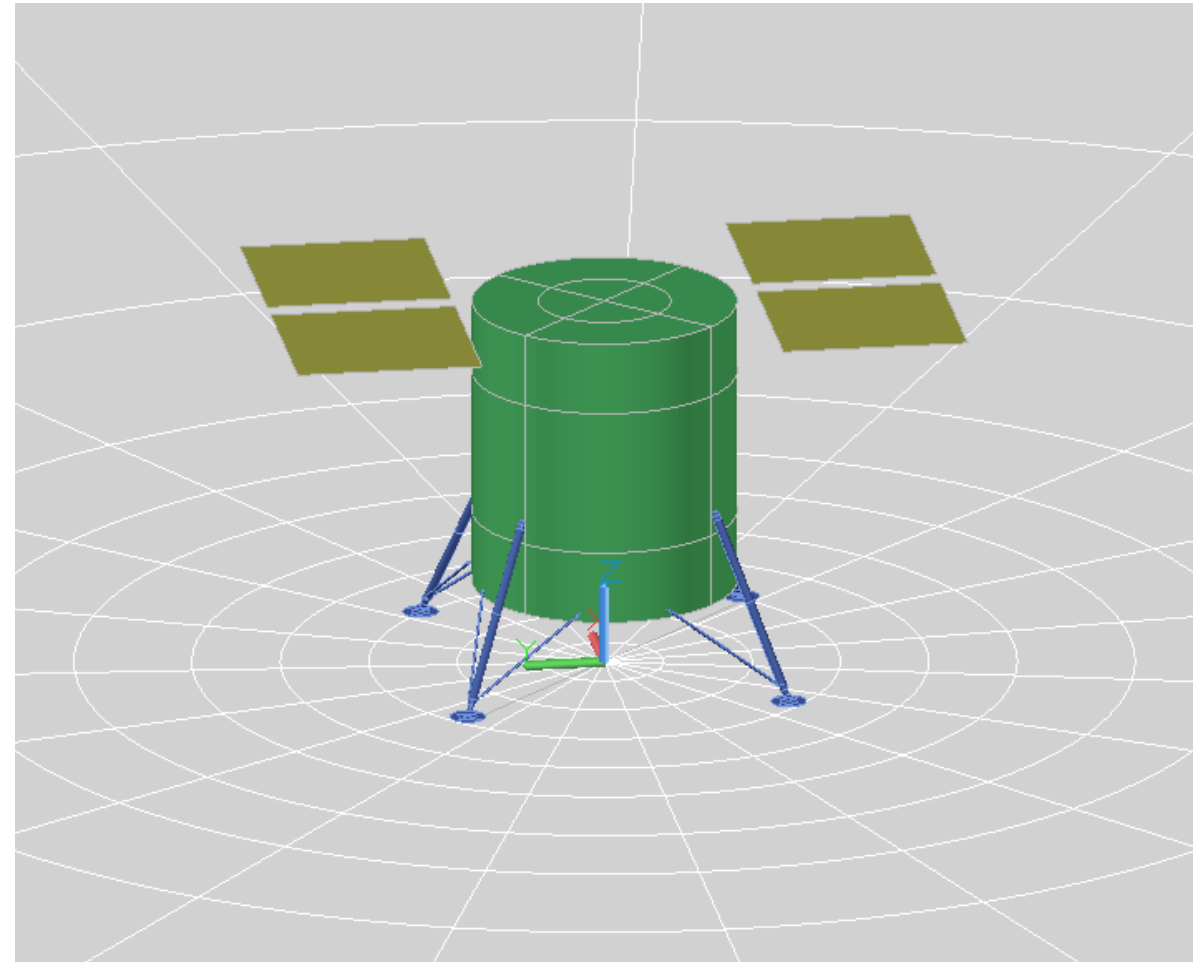
■ Lander Module:

- Main structure is an enclosed cylinder: 4.5m diameter, 5m tall.
- The walls are convectively coupled to a 20°C bulk gas node.
- Lander legs position the main cylinder ~1.5m off the ground.
- The main goal of the lander is to create reasonable and realistic shadows/reflections on the regolith.

■ Optical properties:

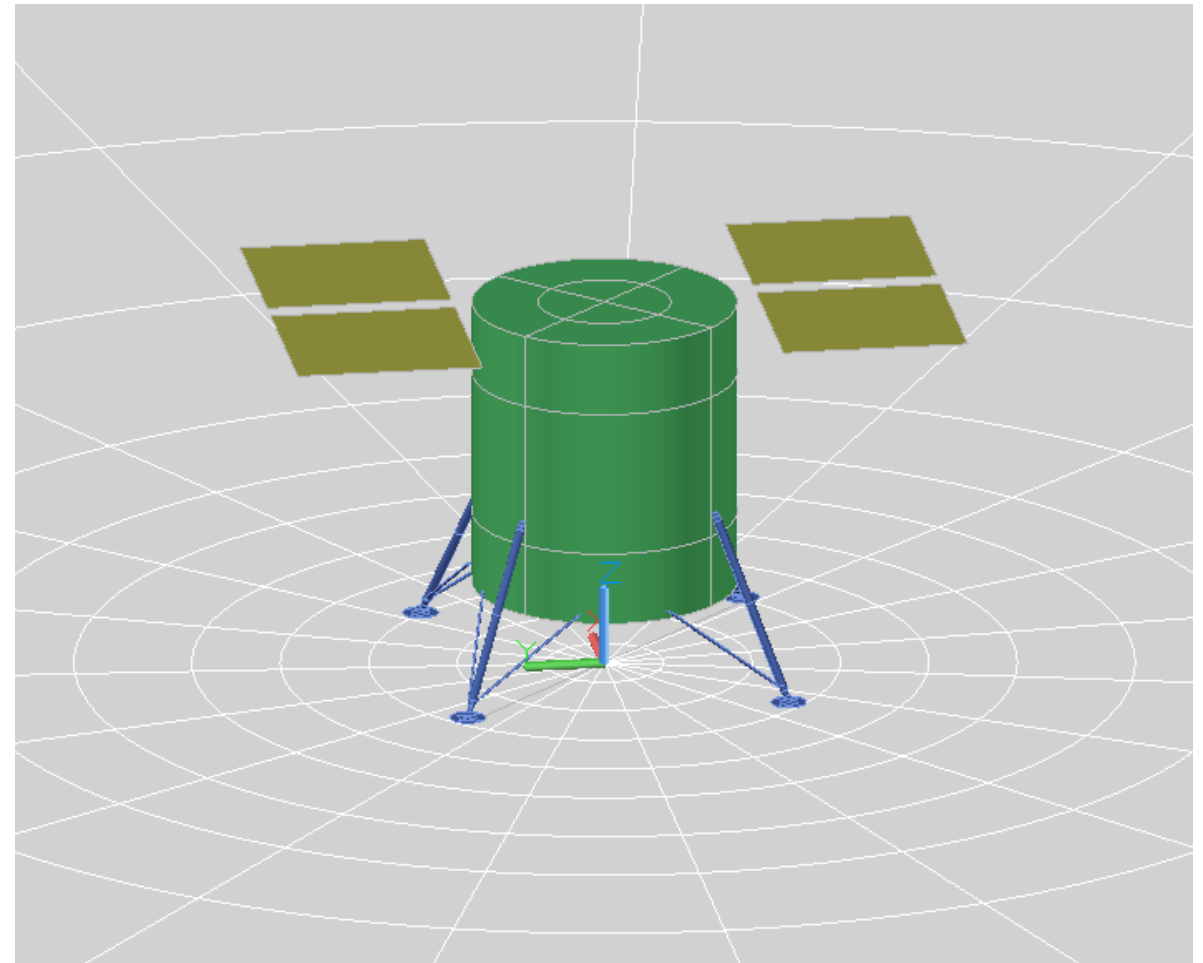
- Cylindrical Structure: Beta Cloth ($\alpha/\epsilon=0.3/0.9$).
- Lander legs: Silver Teflon ($\alpha/\epsilon=0.08/0.81$).
- Radiator top/out: Generic low absorptance white paint ($\alpha/\epsilon=0.09/0.91$) [3].
- Radiator bottom/in: Not in analysis (note underside conditions are studied in Part 2).
- Regolith: Highland optical properties used are: $\alpha/\epsilon = 0.84/0.98$, and mare optical properties used are $\alpha/\epsilon = 0.93/0.98$ [4].

Note: regolith optical properties used are consistent with the regolith type found at each site.



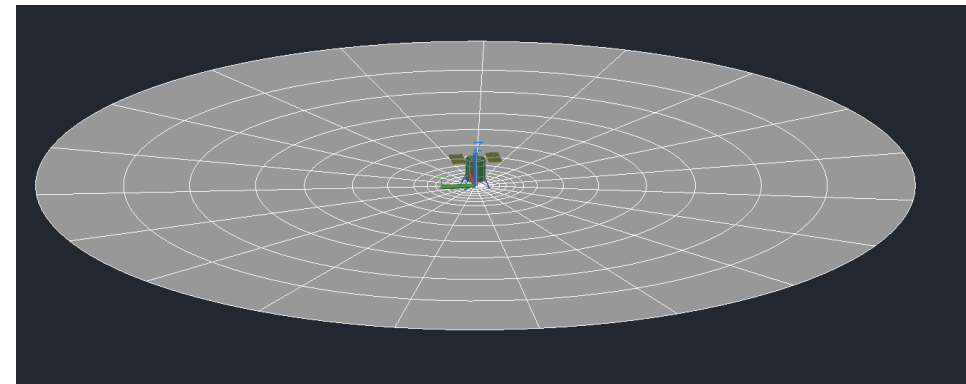
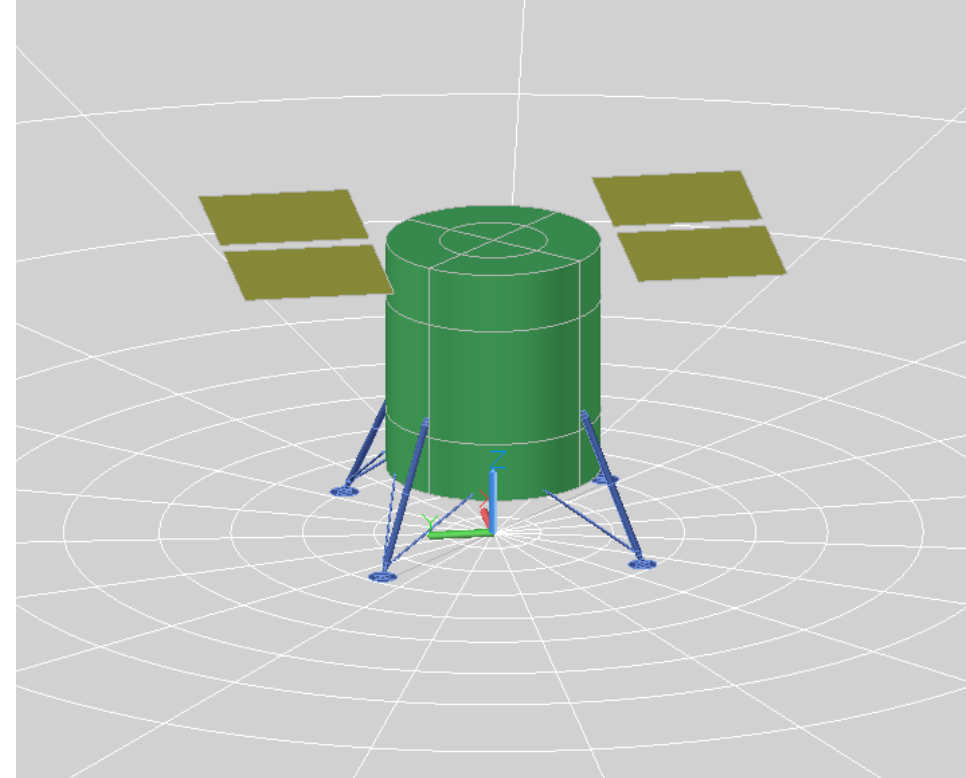
- Thermophysical properties:
 - Lander structure, legs, and radiators: 6061 T6 Aluminum.
 - Regolith: thermophysical properties obtained from the Human Landing System (HLS) Lunar Thermal Analysis Guidebook (LTAG) [5].
- Insulation:
 - Lander structure: $\epsilon^*=0.01$.
 - Lander legs: $\epsilon^*=0.03$.
 - Regolith: Regolith depth & thermal mass is modeled using insulation stack applied to the back/under side (per LTAG recommendation) [5].

Layer #	Thickness (m)	Density (kg/m ³)
Layer 1	0.2614	1723
Layer 2	0.3369	1723
Layer 3	0.504	1800
Layer 4	0.8877	1800



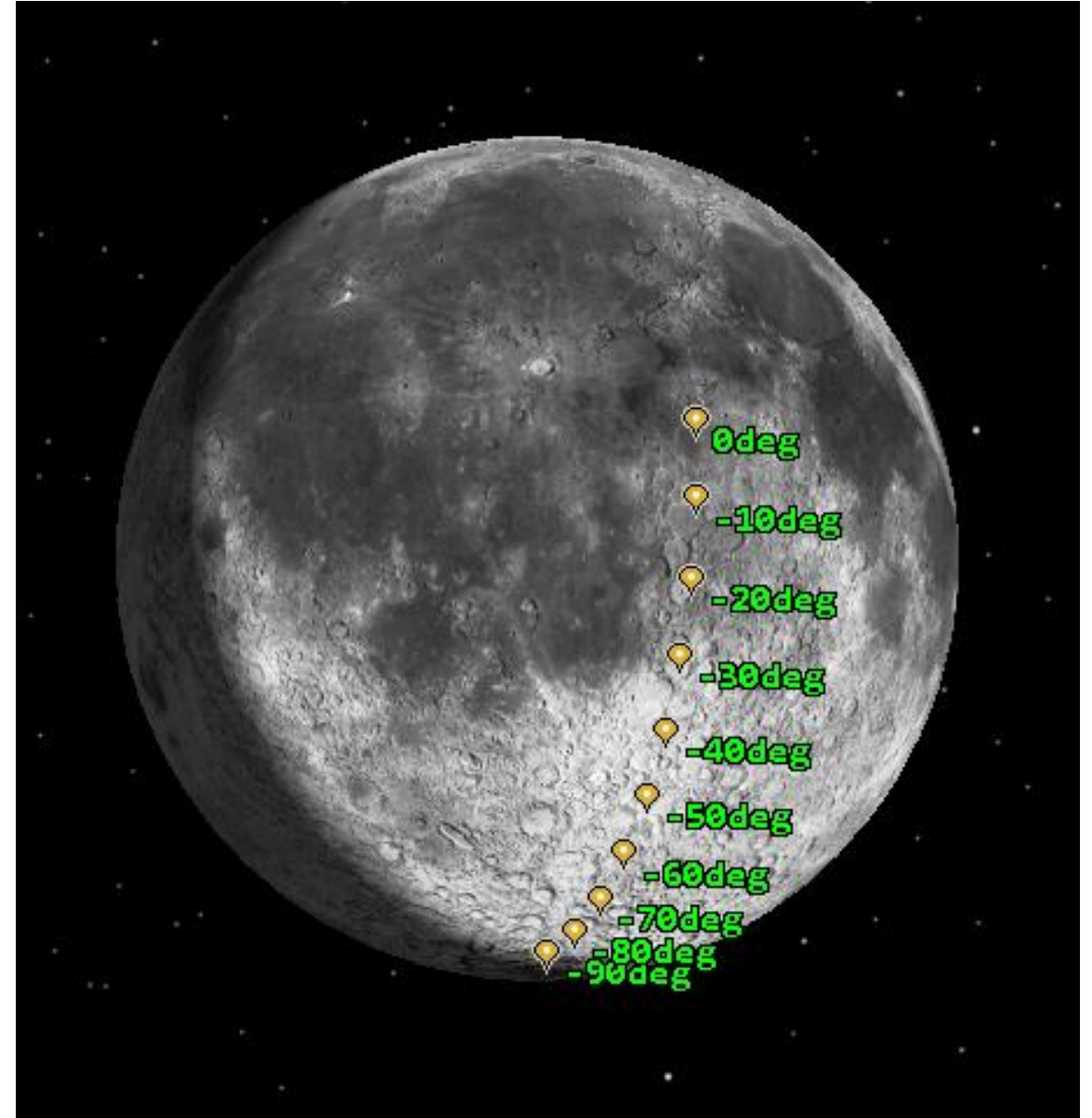
Flat Disk Terrain Standin:

- A perfectly flat disk is used to represent the terrain because:
 - This allows results to be decoupled from location-specific terrain effects.
 - The degradation of radiator performance vs latitude due to underside coatings is dominated by the temperature of the ground directly under the lander which is weakly affected by terrain effects (assuming level ground beneath the lander).
- The radius of the disk is 100m, calculated to achieve 95% of the view factor to an infinite plane.
- **All cases are analyzed separately with Mare and Highland optical properties and results are compared.**
- Regolith depth & thermal mass is modeled using insulation stack applied to the back/under side (per LTAG recommendation)



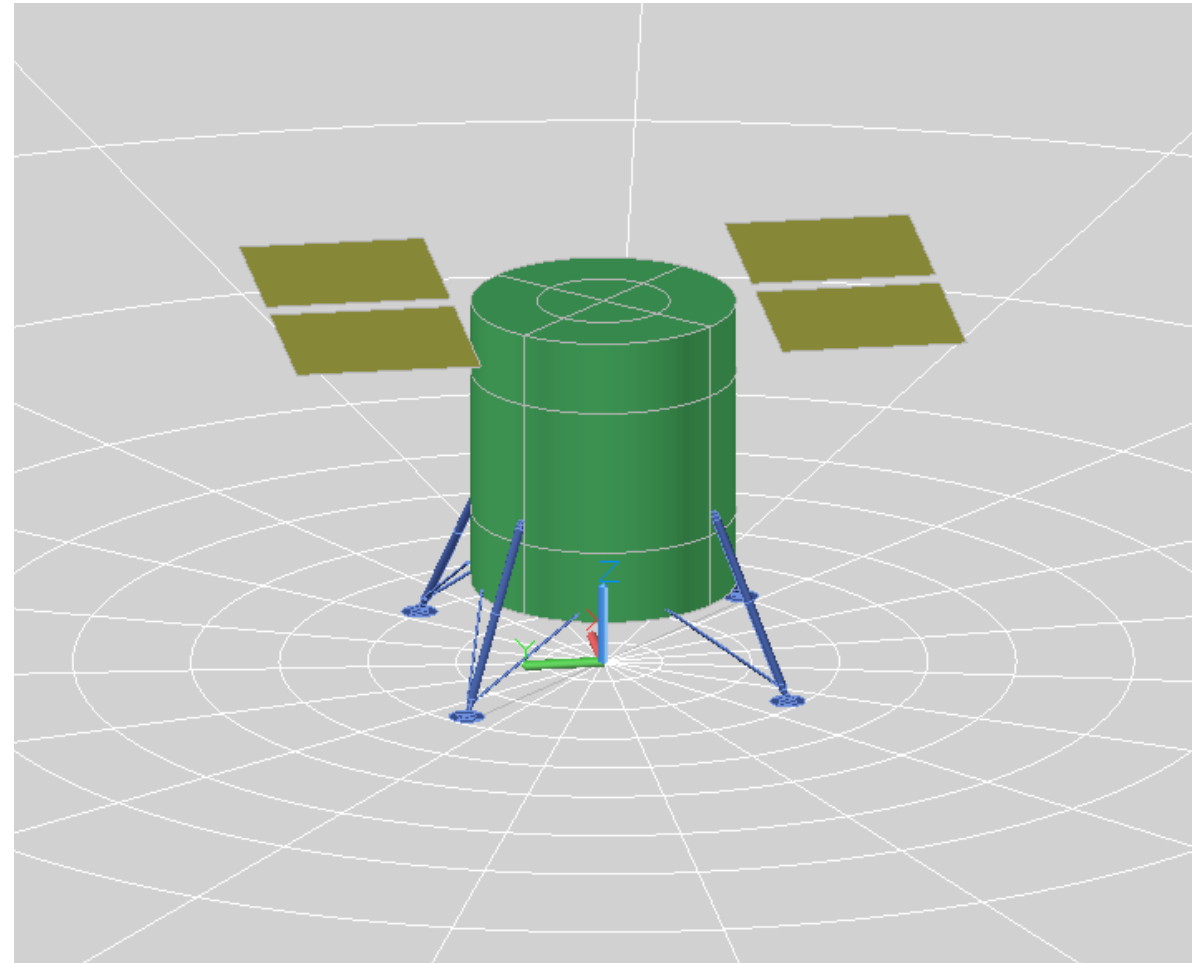
■ Solar Path:

- Though no terrain data is used, STK is used to obtain solar AER (azimuth, elevation, and range) for the specific latitudes and longitudes of interest.
- Longitude is 0° for all 10 sites.
- Latitude is varied from 0° to -90° in 10° increments.
- For each latitude, two solar environments/ case sets are considered:
 - **Transient Initializer:** Approximately 2 years of coarse (48 hour) solar position data that allows the top layer of the regolith to reach dynamic equilibrium. Ends when the lunar day of interest begins.
 - **Lunar Day:** 1 full lunar day at 1-hour increments. The lunar day chosen is common to all latitude cases and was chosen to be at a point where the solar angle of obliquity is nearly 0° .

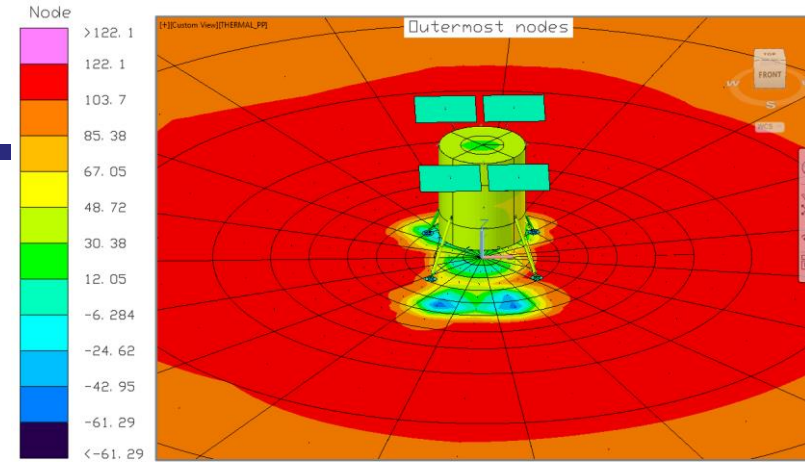
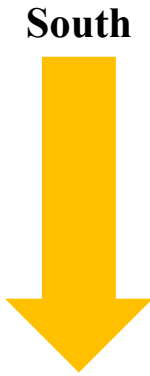


■ Radiators:

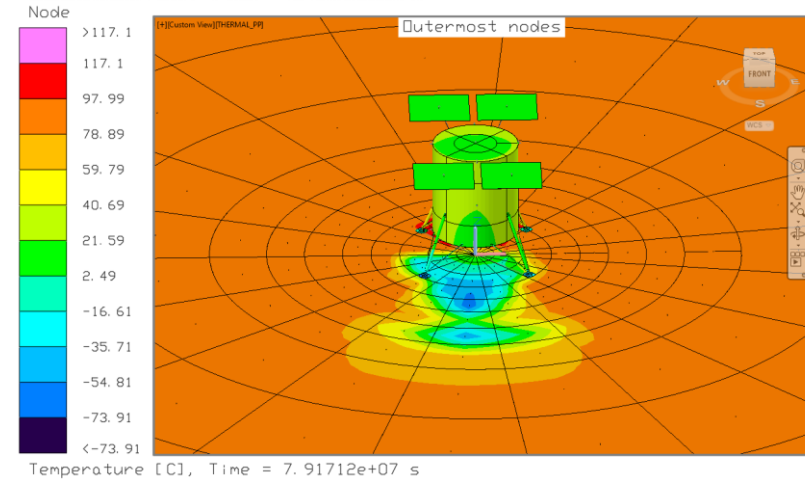
- All radiators are 10m^2 ($3.162\text{m} \times 3.162\text{m}$).
- Four horizontal coplanar radiators are modeled simultaneously in an array around the module:
 - **No Underside Radiation:** Radiation calculations are turned off for the underside. This will serve as a baseline against which the other underside coatings can be compared.
 - **Underside MLI:** Underside is covered with MLI ($\epsilon^*=0.01$) with an outer coating of Silver Teflon ($\alpha/\epsilon=0.08/0.81$).
 - **Low ϵ Coating:** Underside is assumed to be iridite (chromate conversion coating) on aluminum ($\alpha/\epsilon=0.24/0.04$).
 - **High ϵ Coating:** Underside is assumed to be coated with the same coating as the topside, i.e. low absorptance white paint ($\alpha/\epsilon=0.09/0.91$) [3].



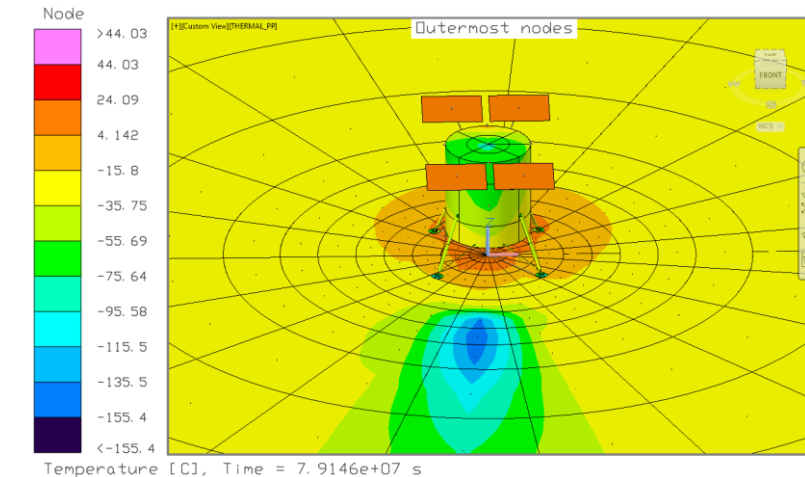
- The farther south the latitude, the more of a southerly shadow the lander will cast at noon (peak solar heating)
- This results in the north side of the vehicle being warmer in almost all cases



-10° Latitude



-40° Latitude



-80° Latitude

Analysis Structure:

Two radiator configurations considered:

- Configuration A:
 - The radiators with underside MLI and no underside radiation are on the **north** side of the vehicle.
 - The High ϵ and Low ϵ underside coated radiators are on the **south** side of the vehicle.
- Configuration B:
 - The High ϵ and Low ϵ underside coated radiators are on the **north** side of the vehicle.
 - The radiators with underside MLI and no underside radiation are on the **south** side of the vehicle.

Two radiator temperatures are considered:

- 60° C (333K)
- 10° C (283K)

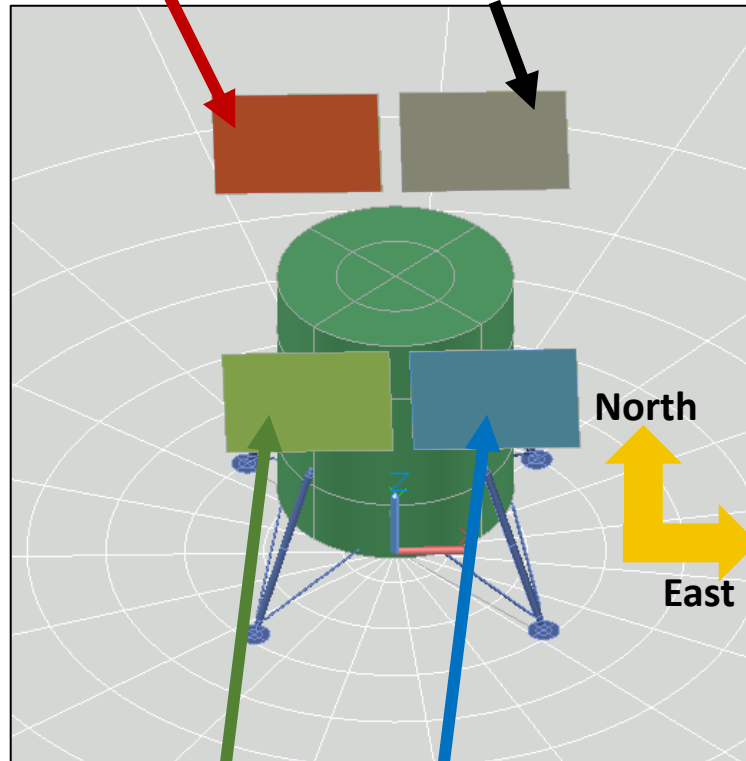
Two regolith optical properties considered:

- Highland
- Mare

- In total, 80 cases are analyzed: one for each configuration, temperature, regolith type, and latitude.

Configuration A

Underside MLI No Underside Radiation

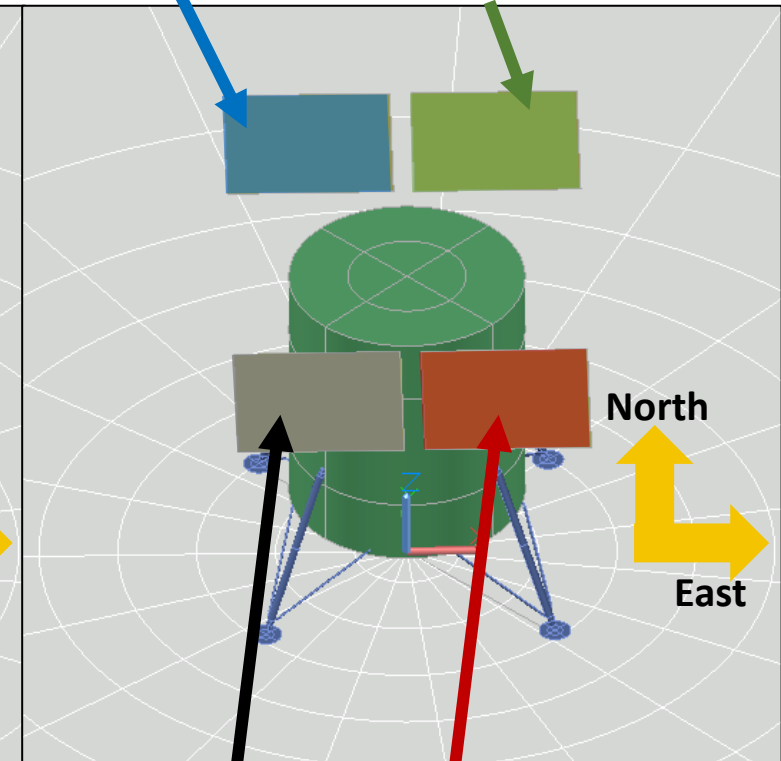


High ϵ Underside Coating

Low ϵ Underside Coating

Configuration B

Low ϵ Underside Coating High ϵ Underside Coating



No Underside Radiation

Underside MLI



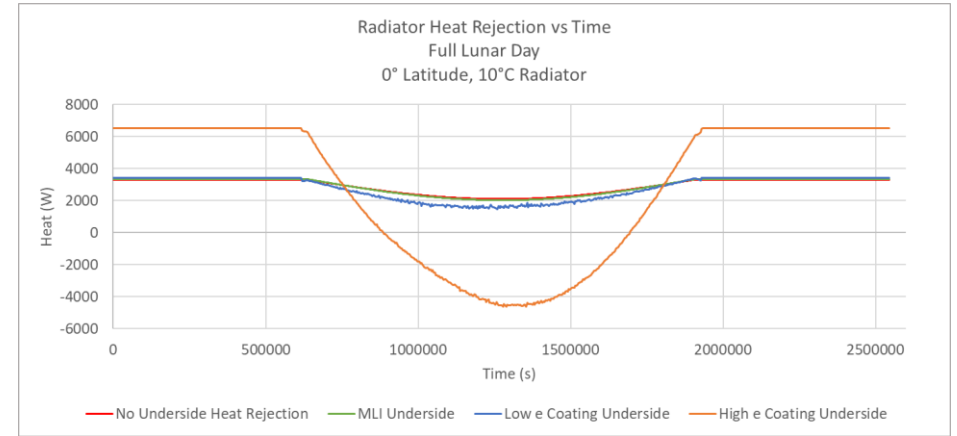
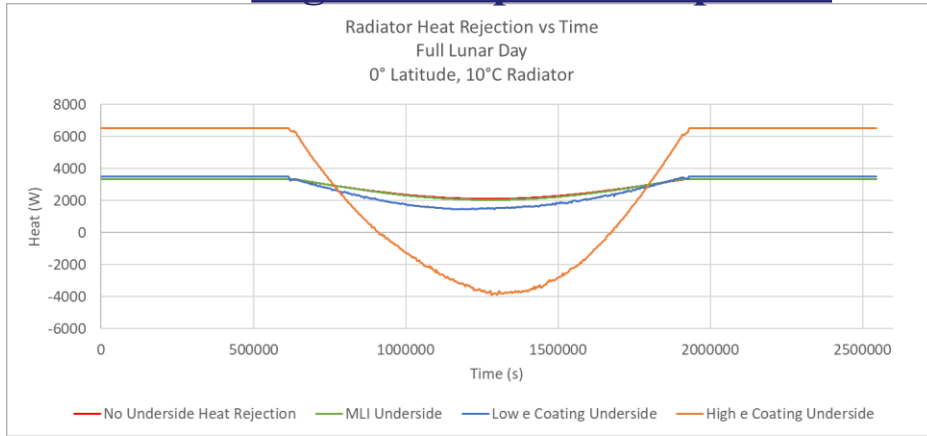
0° Latitude, Full Lunar Day, 10° C Radiators



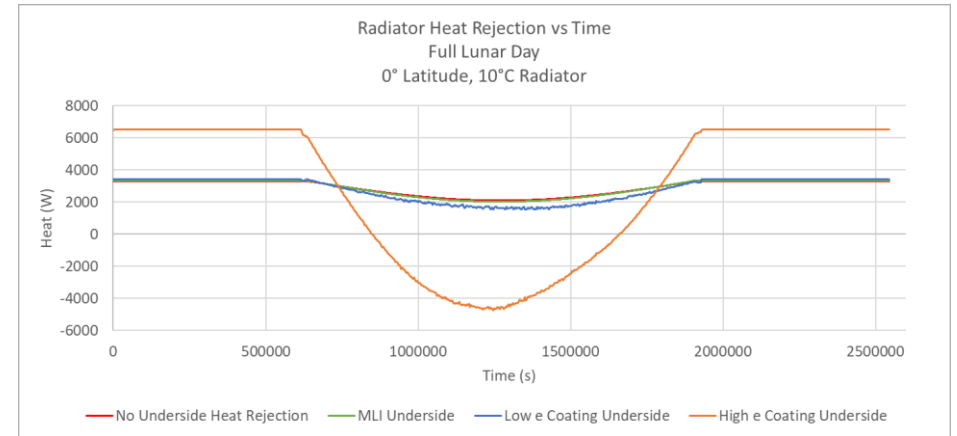
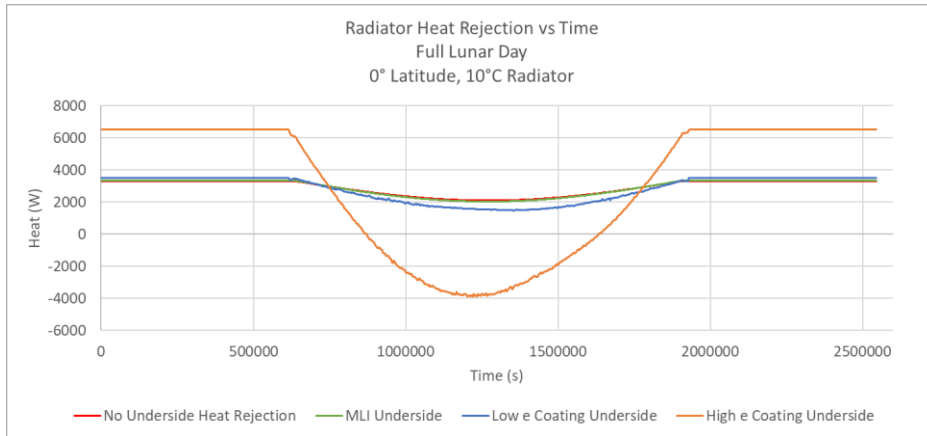
Highland Optical Properties

Mare Optical Properties

CONFIG A



CONFIG B



	CONFIG A: Min Heat Rejection (W)	CONFIG B: Min Heat Rejection (W)
No Underside Radiation	209.7	209.7
Underside MLI	203.2	203.3
Low ε Underside Coating	145.6	147.9
High ε Underside Coating	-388.0	-390.1

	CONFIG A: Min Heat Rejection (W)	CONFIG B: Min Heat Rejection (W)
No Underside Radiation	209.7	209.7
Underside MLI	202.4	202.4
Low ε Underside Coating	146.9	152.6
High ε Underside Coating	-462.2	-474.7

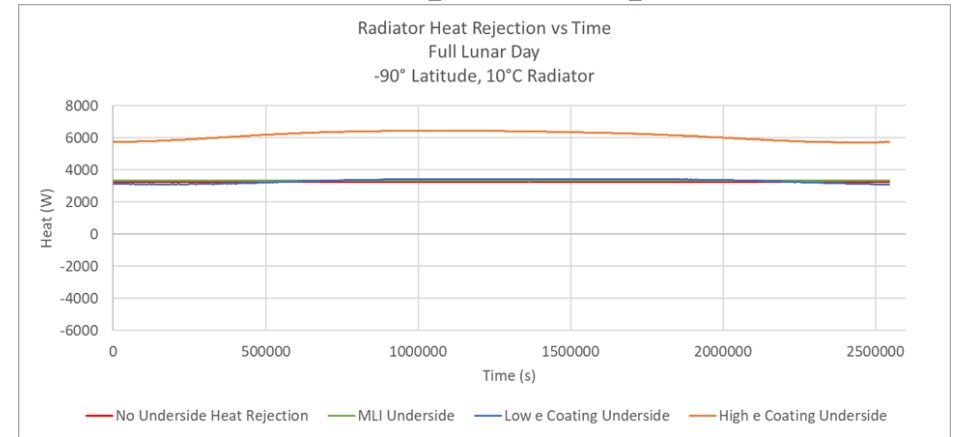
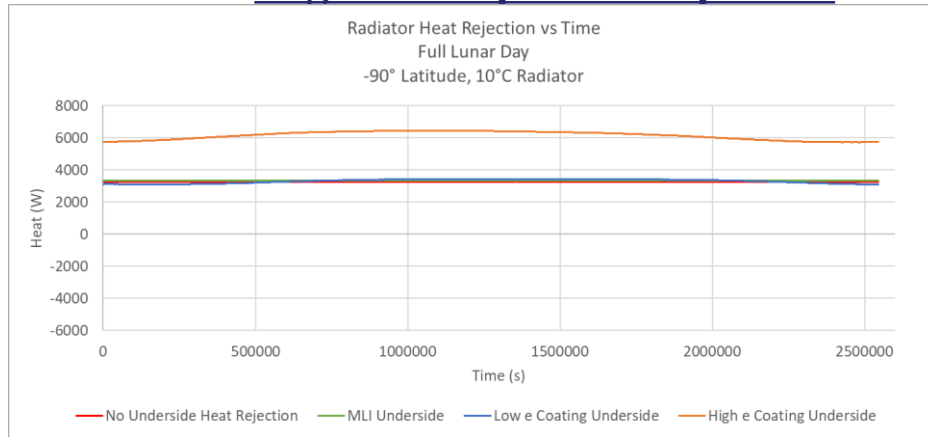


-90° Latitude, Full Lunar Day, 10° C Radiators

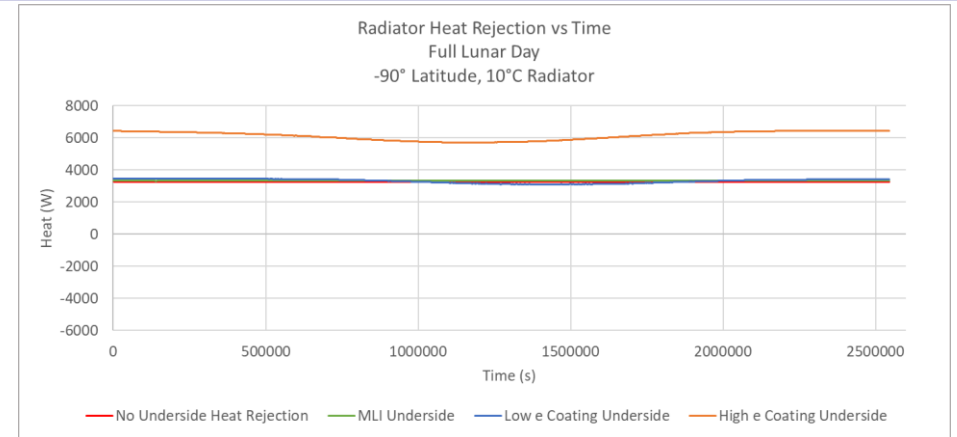
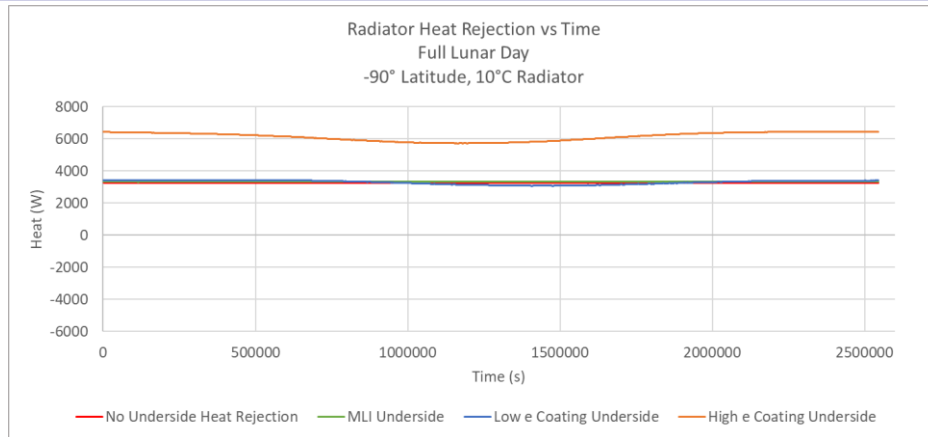
Highland Optical Properties

Mare Optical Properties

**CONFIG
A**



**CONFIG
B**



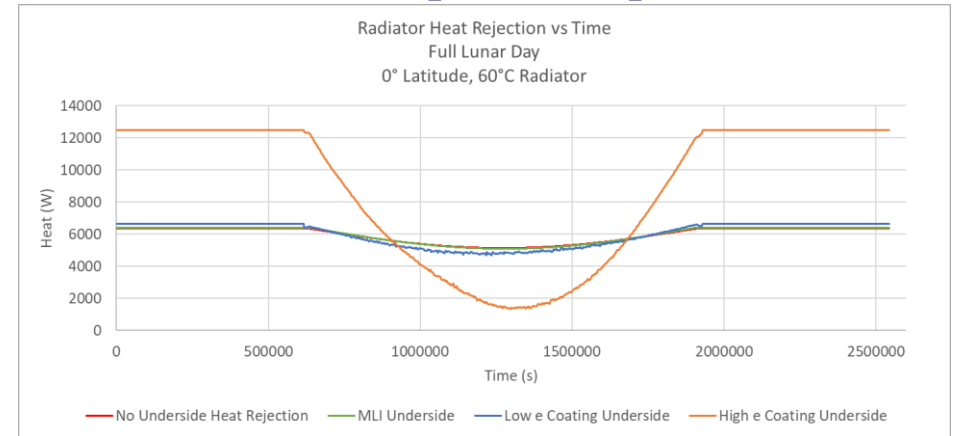
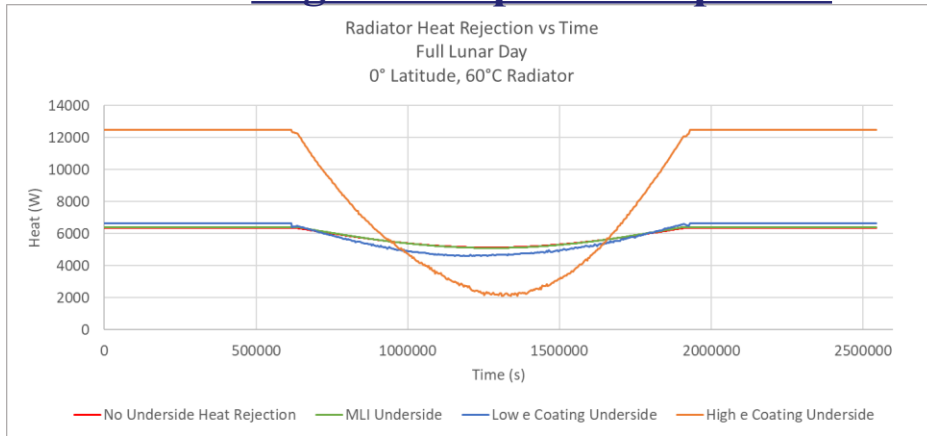
	CONFIG A: Min Heat Rejection (W/m ²)	CONFIG B: Min Heat Rejection (W/m ²)
No Underside Radiation	331.5	331.5
Underside MLI	334.2	334.2
Low ε Underside Coating	307.9	306.9
High ε Underside Coating	572.6	572.1

	CONFIG A: Min Heat Rejection (W/m ²)	CONFIG B: Min Heat Rejection (W/m ²)
No Underside Radiation	331.5	331.5
Underside MLI	334.2	334.2
Low ε Underside Coating	308.9	308.8
High ε Underside Coating	570.8	570.4

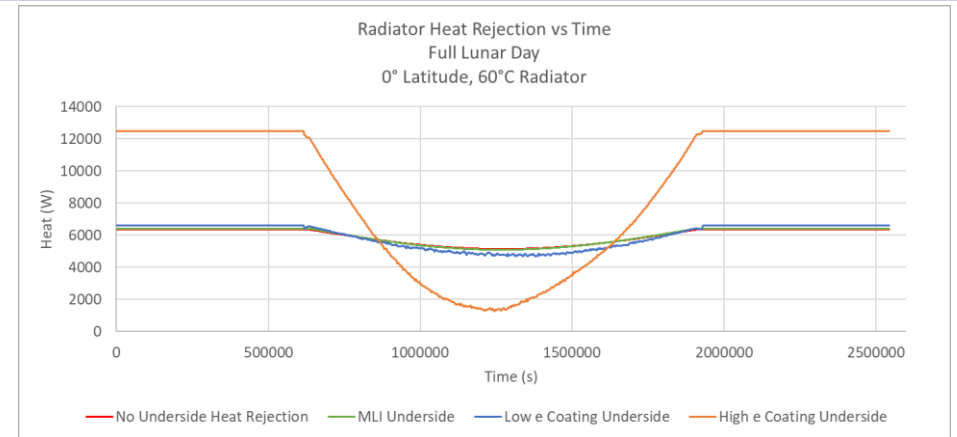
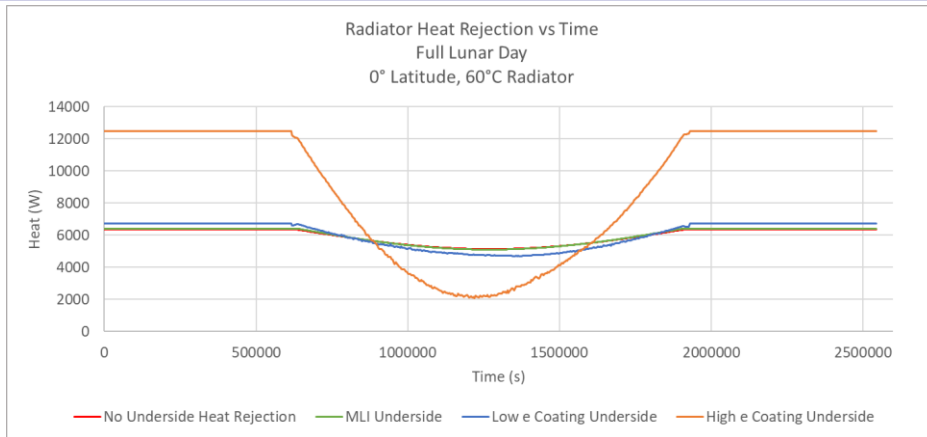
Highland Optical Properties

Mare Optical Properties

CONFIG A



CONFIG B



	CONFIG A: Min Heat Rejection (W)	CONFIG B: Min Heat Rejection (W)
No Underside Radiation	5134	5134
Underside MLI	5102	5102
Low ϵ Underside Coating	4593	4692
High ϵ Underside Coating	2102	2087

	CONFIG A: Min Heat Rejection (W)	CONFIG B: Min Heat Rejection (W)
No Underside Radiation	5134	5134
Underside MLI	5093	5093
Low ϵ Underside Coating	4690	4679
High ϵ Underside Coating	1349	1246



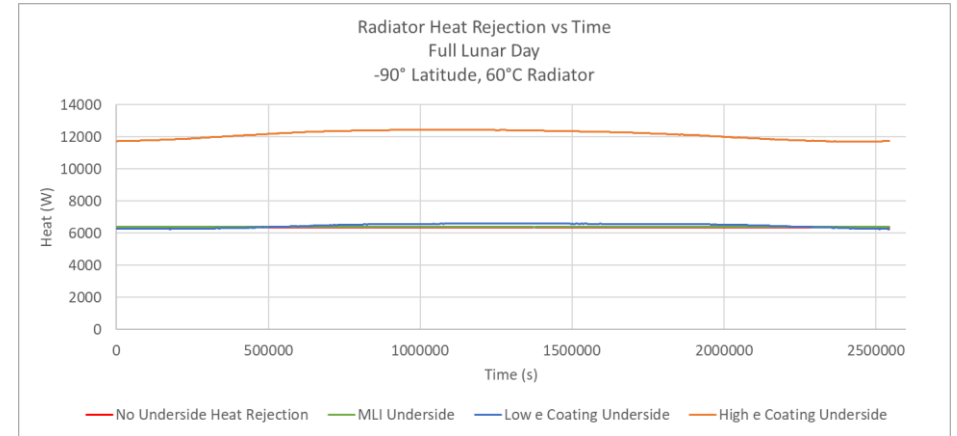
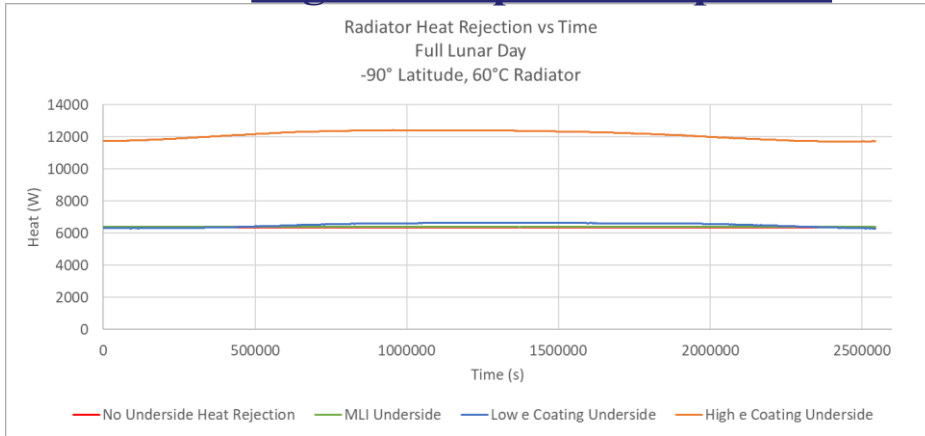
-90° Latitude, Full Lunar Day, 60° C Radiators



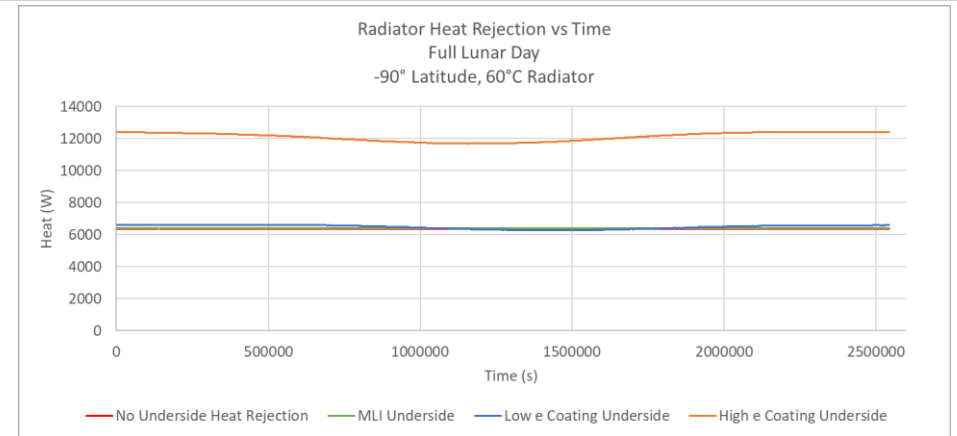
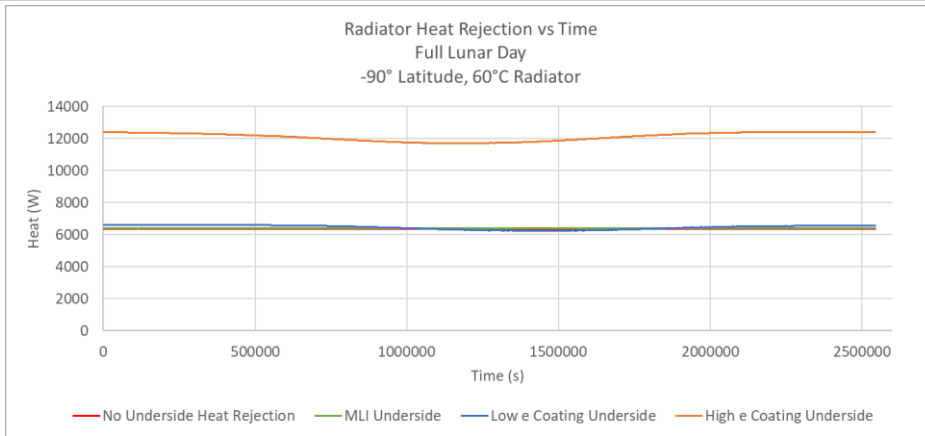
Highland Optical Properties

Mare Optical Properties

**CONFIG
A**



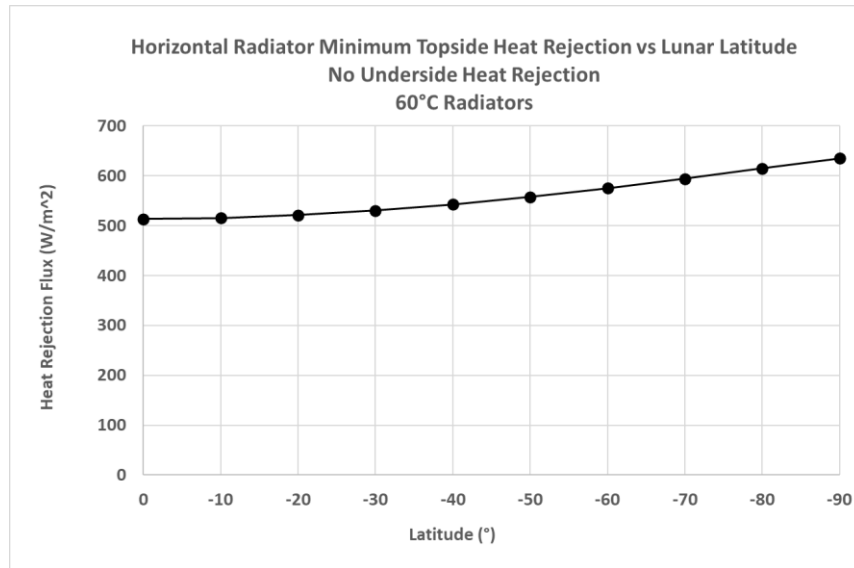
**CONFIG
B**



	CONFIG A: Min Heat Rejection (W/m ²)	CONFIG B: Min Heat Rejection (W/m ²)
No Underside Radiation	6352	6352
Underside MLI	6411	6411
Low ε Underside Coating	6290	6229
High ε Underside Coating	11701	11698

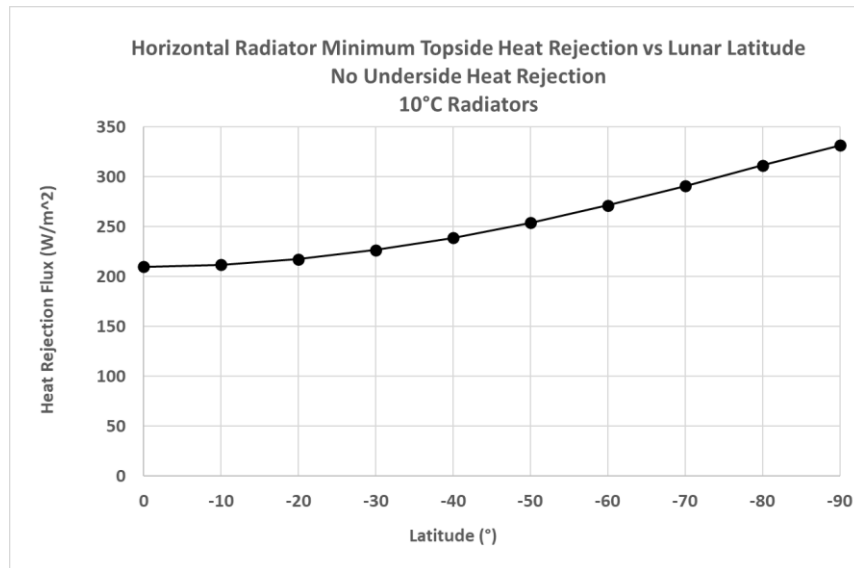
	CONFIG A: Min Heat Rejection (W/m ²)	CONFIG B: Min Heat Rejection (W/m ²)
No Underside Radiation	6352	6352
Underside MLI	6411	6411
Low ε Underside Coating	6251	6261
High ε Underside Coating	11704	11683

60° C Radiator



Latitude (°)	Minimum (Noon) Topside Heat Rejection (W/m ²)
0	513
-10	515
-20	521
-30	530
-40	543
-50	558
-60	575
-70	594
-80	615
-90	635

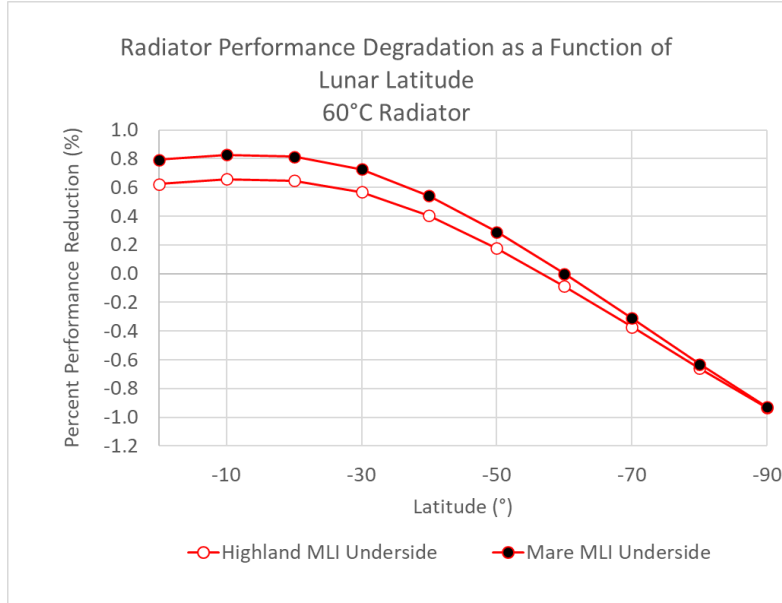
10° C Radiator



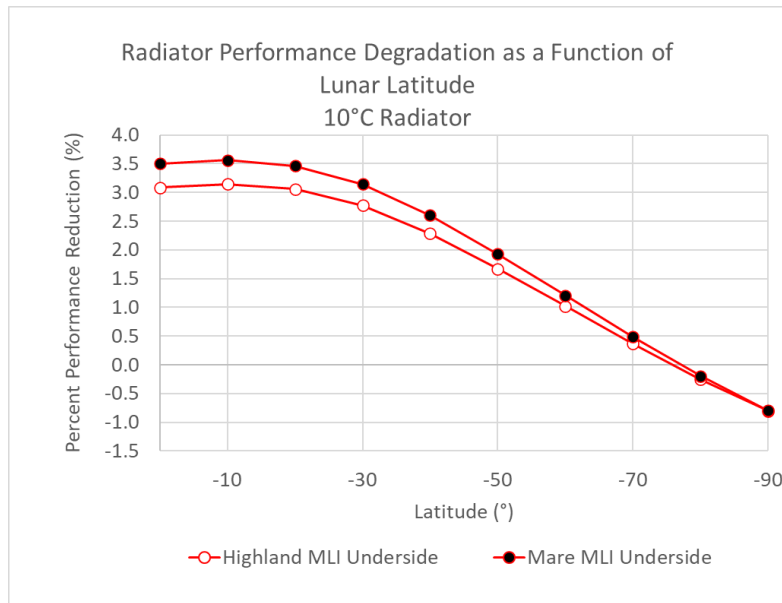
Latitude (°)	Minimum (Noon) Topside Heat Rejection (W/m ²)
0	210
-10	212
-20	217
-30	227
-40	239
-50	254
-60	271
-70	291
-80	311
-90	332

- Minimum (noon) radiator topside heat rejection decreases steadily with lunar latitude due to the increasingly shallow angle to the sun resulting in decreased solar energy deposition per unit area.
- Neglecting terrain effects and underside heat rejection, a horizontal radiator at noon on the south pole rejects 122W/m² more than a horizontal radiator at noon on or near the equator regardless of temperature.
- Note that radiator heat rejection **change** with latitude is independent of radiator temperature because solar flux is the same regardless of radiator temperature.
- While the heat rejection **change** vs latitude is not a function of radiator temperature, the absolute heat rejected is a function of temperature. On average a 60° C radiator rejects 304W/m² more than a 10° C radiator, regardless of latitude.

60° C Radiator North Side Degradation



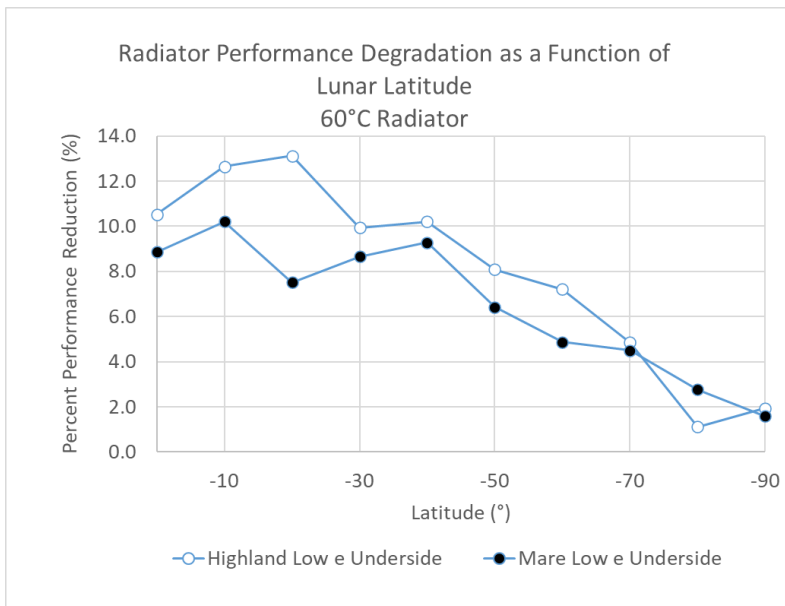
10° C Radiator North Side Degradation



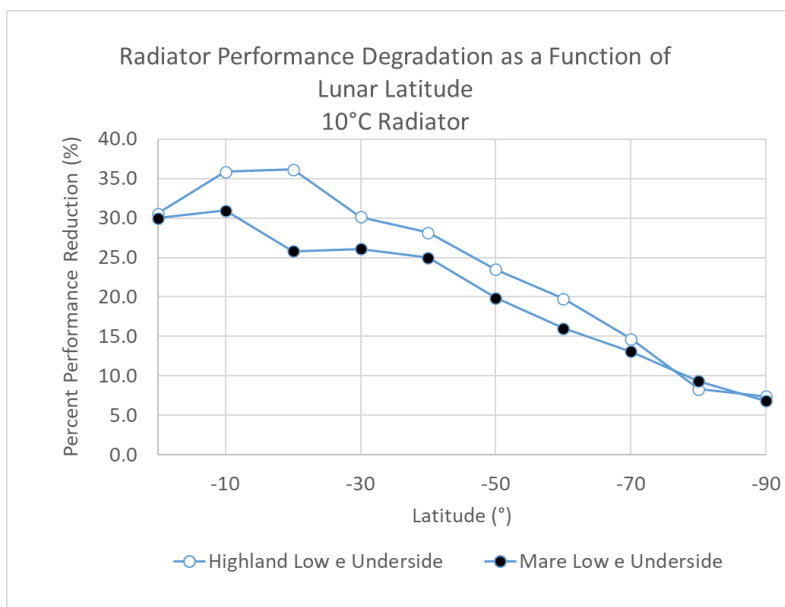
***NOTE:**
Performance degradation is calculated from *minimum* (noon) radiator heat rejection

- MLI with an $\epsilon^*=0.01$ applied to the underside results in minimal radiator performance degradation at all latitudes regardless of radiator temperature.
- With underside MLI, Highland and Mare radiator performance is very similar.
- The latitude at which no heat is absorbed or rejected by the backside is:
 - **60° C Radiator:** -57° for Highland and -60° for Mare on the north (hottest) side of the lander.
 - **10° C Radiator:** -76° for Highland and -77° for Mare on the north (hottest) side of the lander.

60° C Radiator North Side Degradation



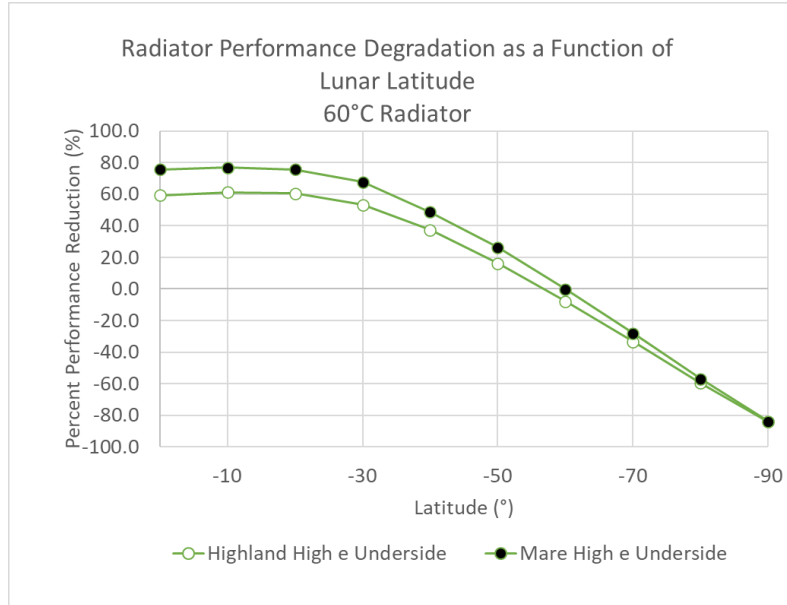
10° C Radiator North Side Degradation



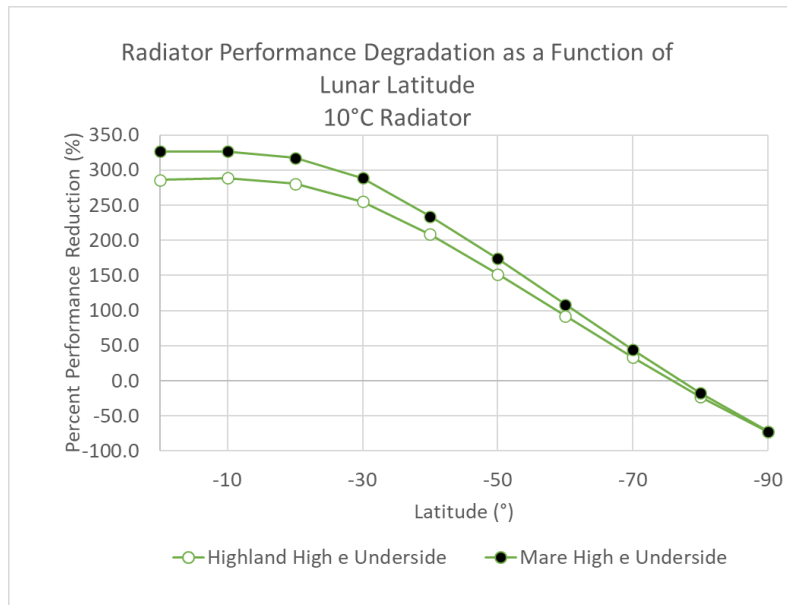
***NOTE:**
Performance degradation is calculated from *minimum (noon)* radiator heat rejection

- Note the noise in the data is due to a 2% “total absorbed” error in heat rate calculations – this is normally more than sufficient, however the low ϵ^* coating exacerbates the error.
- Worst case equatorial performance reduction can be as high as ~36% for 10°C radiators and ~13% for 60°C radiators.
- Due to the noise in this data, the effects of low emissivity underside coatings should be considered inconclusive.

60° C Radiator North Side Degradation

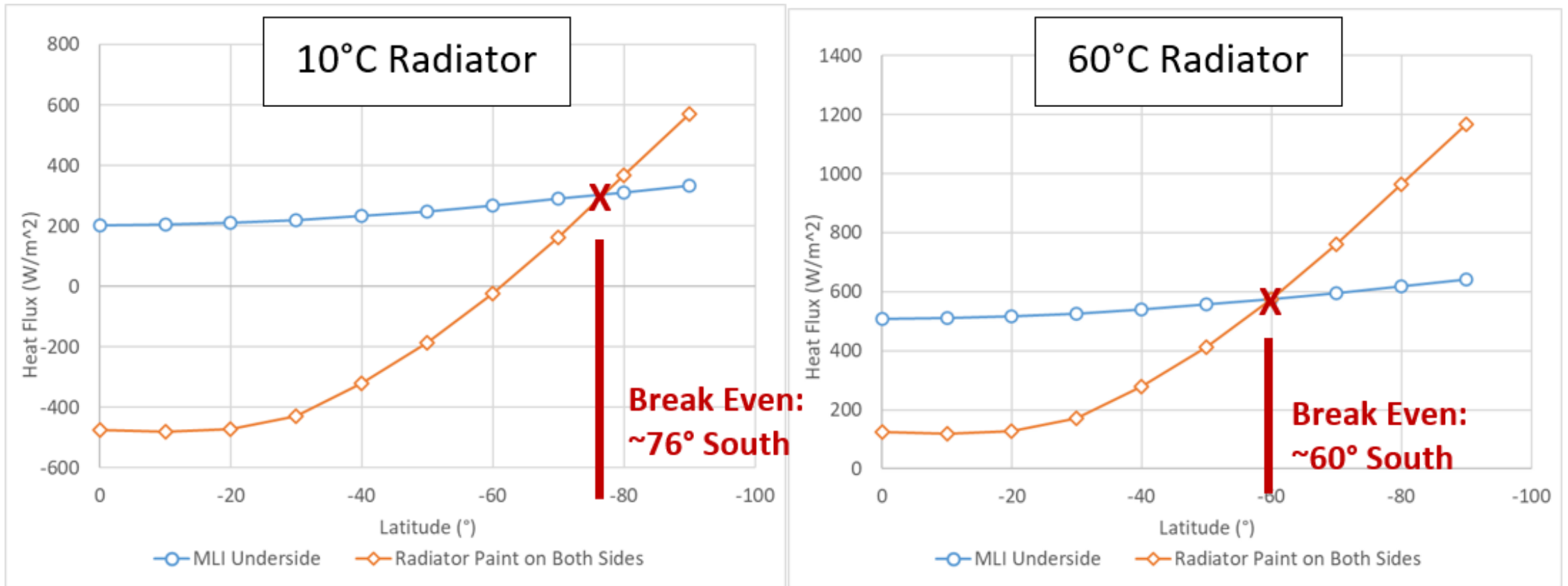


10° C Radiator North Side Degradation



***NOTE:**
Performance degradation is calculated from *minimum (noon) radiator heat rejection*

- The latitude at which radiator performance degradation is greater than 100% (i.e. in total the radiator is *absorbing* heat) is:
 - **60° C Radiator:** None – the warmer radiator can reject heat at all lunar latitudes.
 - **10° C Radiator:** -59° for Highland and -61° for Mare on the north (hottest) side of the lander.
- Heat is rejected rather than absorbed by the underside (i.e. the underside improves radiator performance) at latitudes south of:
 - **60° C Radiator:** -57° for Highland and -60° for Mare on the north (hottest) side of the lander.
 - **10° C Radiator:** -76° for Highland and -77° for Mare on the north (hottest) side of the lander.
- At the south pole, a double-sided radiator can result in:
 - **60° C Radiator:** 84% increase in heat rejection or an additional ~535W/m².
 - **10° C Radiator:** 73% increase in heat rejection or an additional ~240W/m².



There is a breakeven point in latitude at which the heat rejection from a radiator with a high emissivity underside coating equals that of a radiator that is insulated on the underside. South of this point, the radiator with a high emissivity coating on the underside offers superior performance.

10° C Radiator Performance Degradation Factors

Latitude	Worst Case Performance Degradation Due to Latitude and Underside Condition: <u>MLI Underside Covering</u>		Worst Case Performance Degradation Due to Latitude and Underside Condition: <u>Low Emissivity Underside Coating</u>		Worst Case Performance Degradation Due to Latitude and Underside Condition: <u>High Emissivity Underside Coating</u>	
	Highland	Mare	Highland*	Mare*	Highland	Mare
0°	3.1%	3.5%	30.6%	30.0%	286.0%	326.4%
-10°	3.1%	3.6%	35.8%	31.0%	288.8%	326.4%
-20°	3.1%	3.5%	36.1%	25.8%	280.4%	317.6%
-30°	2.8%	3.1%	30.1%	26.1%	255.1%	288.8%
-40°	2.3%	2.6%	28.2%	25.0%	208.5%	234.1%
-50°	1.7%	1.9%	23.5%	19.9%	151.9%	173.8%
-60°	1.0%	1.2%	19.8%	16.0%	92.0%	108.8%
-70°	0.4%	0.5%	14.7%	13.1%	33.4%	44.2%
-80°	-0.3%	-0.2%	8.3%	9.3%	-23.0%	-17.6%
-90°	-0.8%	-0.8%	7.4%	6.9%	-72.6%	-72.0%

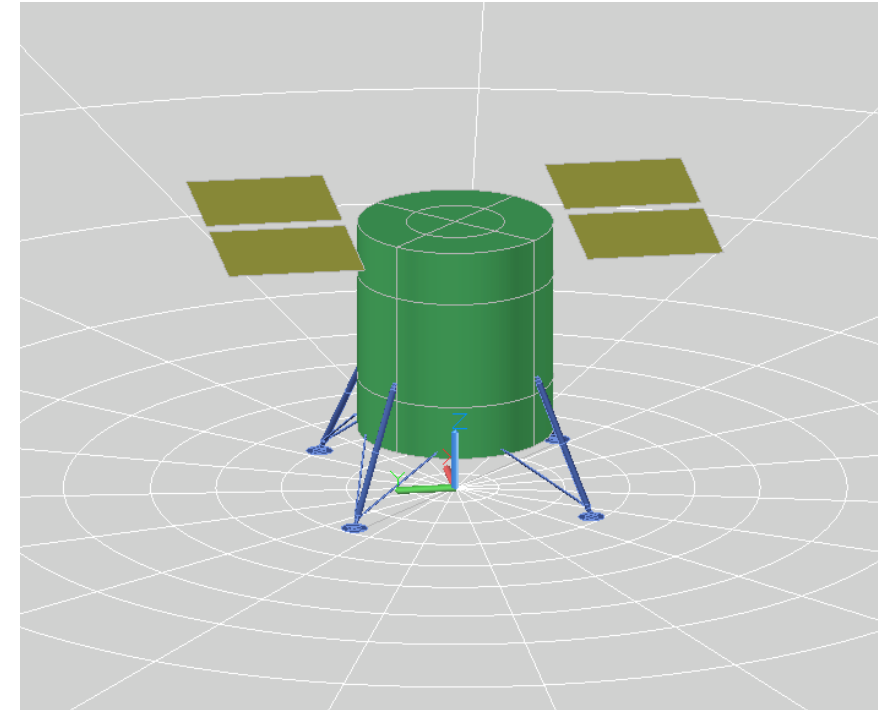
* Low emissivity performance degradation data is inconclusive due to the noise observed.

60° C Radiator Performance Degradation Factors

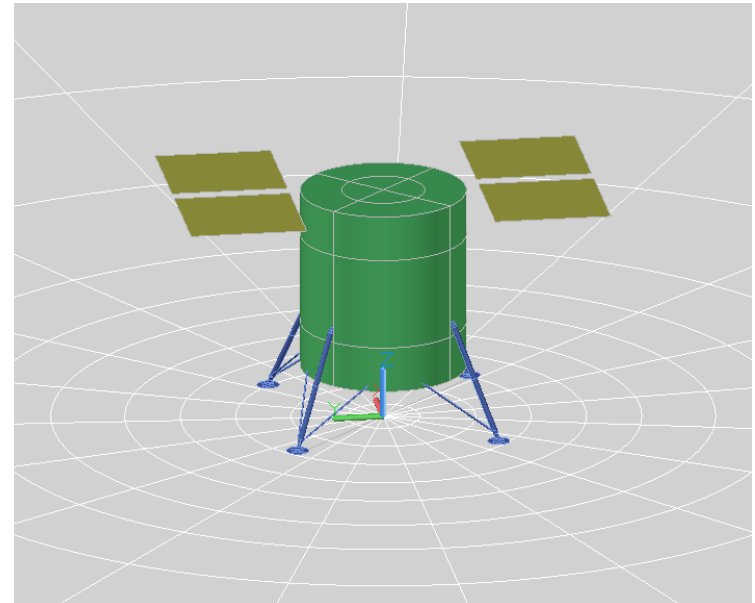
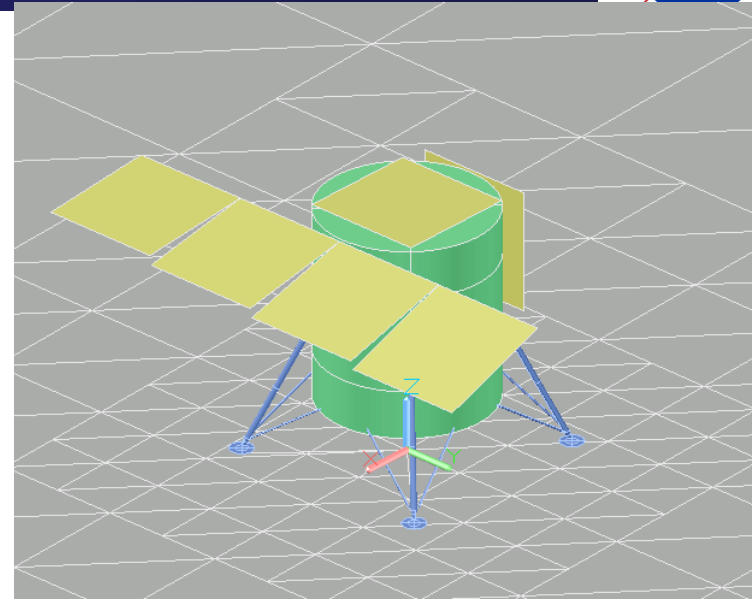
Latitude	Worst Case Performance Degradation Due to Latitude and Underside Condition: <u>MLI Underside Covering</u>		Worst Case Performance Degradation Due to Latitude and Underside Condition: <u>Low Emissivity Underside Coating</u>		Worst Case Performance Degradation Due to Latitude and Underside Condition: <u>High Emissivity Underside Coating</u>	
	Highland	Mare	Highland*	Mare*	Highland	Mare
0°	0.6%	0.8%	10.5%	8.9%	59.4%	75.7%
-10°	0.7%	0.8%	12.7%	10.2%	61.3%	76.8%
-20°	0.6%	0.8%	13.1%	7.5%	60.4%	75.7%
-30°	0.6%	0.7%	9.9%	8.7%	53.3%	67.8%
-40°	0.4%	0.5%	10.2%	9.3%	37.4%	48.8%
-50°	0.2%	0.3%	8.1%	6.4%	16.2%	26.2%
-60°	-0.1%	0.0%	7.2%	4.9%	-7.8%	-0.2%
-70°	-0.4%	-0.3%	4.9%	4.5%	-33.3%	-28.0%
-80°	-0.7%	-0.6%	1.1%	2.8%	-59.5%	-56.8%
-90°	-0.9%	-0.9%	1.9%	1.6%	-84.2%	-83.9%

* Low emissivity performance degradation data is inconclusive due to the noise observed.

1. Neglecting terrain and underside heat transfer, a horizontal radiator can reject $\sim 120\text{W/m}^2$ more on south pole than at the equator regardless of radiator temperature.
2. Unless MLI is used, the performance of horizontal radiators is sensitive to the position relative to the lander shadow. If the radiator is positioned such that the underside has a high field of view to regolith shaded by the lander, the performance can be improved compared to the same radiator positioned on the sun-side of the lander.
3. Applying MLI with $\epsilon^* \leq 0.01$ to the underside of a horizontal radiator serves as an effective insulator even in extreme hot equatorial cases.
4. A low IR emissivity underside coating appears to perform poorly at equatorial latitudes; however, an improved model should be used to draw any definitive conclusions.
5. For a 10°C radiator, a high IR emissivity underside coating was found to be severely detrimental to radiator performance north of -47° or -61° Latitude (depending on the side of the lander and optical properties).
6. Double-sided radiators were found to perform better than MLI-backed horizontal radiators south of -76° Latitude for 10°C radiators and south of -60° Latitude for 60°C radiators.



- Because the two studies were decoupled, degradation factors for latitude and terrain can be applied independently or stacked to estimate the worst-case effects of each parameter on radiator performance anywhere on the lunar surface.
- Note, however, that terrain degradation factors will become more and more conservative the closer the site is located to the poles.
- Due to the narrow focus of this study (10° C to 60° C deployable, horizontal radiators), another hope of this study is to present methods that can be employed to perform analysis of other specific radiator designs.
- Future radiator performance degradation studies using these methods might include:
 - Vertical radiator performance as a function of latitude
 - Unique terrain environments
 - Dust effects as a function of both terrain and latitude
 - Different set temperatures
- While these approximation tools are not a replacement for detailed analysis and will tend toward conservatism, they provide a fast-turnaround design assessment capability that can speed up and improve the accuracy of early mission phase thermal system scaling.





References



- [1] Apollo 11 - NASA. (n.d.). NASA. Retrieved August 7, 2024, from <https://www.nasa.gov/gallery/apollo-11/page/2/>
- [2] Apollo 15 - NASA. (n.d.). NASA. Retrieved August 7, 2024, from <https://www.nasa.gov/gallery/apollo-15/>
- [3] AZW/LA-II Ultra-Low Solar Absorptance White Thermal Control Paint / Coating. (n.d.). AZ Technology LLC. Retrieved August 5, 2024, from <https://www.aztechnology.com/product/2/azw-la-ii>
- [4] Roberts, B. (2019). Cross Program Design Specification for Natural Environments (DSNE), NASA Technical Reports Server. <https://ntrs.nasa.gov/citations/20200000867>
- [5] Human Landing System Lunar Thermal Analysis Guidebook. (2021). National Aeronautics and Space Administration, Baseline Release. https://ntrs.nasa.gov/api/citations/20210010030/downloads/HLS-UG-001%20Lunar%20Thermal%20Analysis%20Guidebook%20Baseline_STI.pdf